Geological Magazine

www.cambridge.org/geo

Taxonomy and palaeoenvironmental distribution of palaeopascichnids

Anton Kolesnikov[1,2] and Vladislav Desiatkin[1,3]

[1]Geological Institute of the Russian Academy of Sciences, Pyzhevsky Lane 7, Moscow 119017, Russia; [2]Institute of the Earth's Crust of the Siberian Branch of the Russian Academy of Sciences, Lermontova Street 128, Irkutsk 664033, Russia and [3]Lomonosov Moscow State University, Leninskie Gory 1, Moscow 119234, Russia

Original Article

Cite this article: Kolesnikov A and Desiatkin V (2022) Taxonomy and palaeoenvironmental distribution of palaeopascichnids. *Geological Magazine* **159**: 1175–1191. https://doi.org/10.1017/S0016756822000437

Received: 7 March 2021
Revised: 17 April 2022
Accepted: 24 April 2022
First published online: 13 June 2022

Keywords:
Ediacaran; Vendian; *Palaeopascichnus*; *Orbisiana*; Ediacaran biota; taxonomy; palaeoecology

Author for correspondence:
Anton Kolesnikov,
Email: kolesnikov@ginras.ru

Abstract

Palaeopascichnida is a problematic group of extinct organisms that is globally distributed in Ediacaran sequences of Avalonia, Baltica, Siberia, South China and Australia. The fossils related to Palaeopascichnida consist of serially or cluster-like arranged, millimetre- to centimetre-scale globular or allantoid chambers, which are characterized by substantial differences in preservation, leading to no consistent diagnosis for these organisms. Here we integrate morphometric variation, stratigraphic distribution and habitat settings of more than 1200 specimens from all known fossil localities. The results of the morphological analysis demonstrate variation in chamber shape and size, and allow us to recognize six valid species within the group. Statistical analysis of the specimen distribution with respect to sedimentary environments indicates a significant difference in palaeoecological settings between species, making a significant contribution to the evolution and systematic palaeontology of these problematic organisms and perspective on their use in Neoproterozoic biostratigraphy. Our revision and systematic study sheds new light on one of the least studied groups of the late Ediacaran biota.

UUID: http://zoobank.org/e7fbba20-ee49-46de-b99a-6d8ee8cbc5b1

1. Introduction

The Ediacaran biota traditionally was interpreted as macroscopic soft-bodied organisms preserved as moulds and casts in sedimentary rock (Waggoner, 2003; Fedonkin *et al.* 2007; Grazhdankin, 2014). Despite the fact that some representatives of this biota may have had various relatively 'hard' and elastic bodies, there was no strong evidence for the presence of skeletal macroscopic organisms in Ediacaran time. Nevertheless, it is recognized that doubtless tubular eumetazoans with biologically controlled mineralization appeared for the first time at the end of the Ediacaran Period prior to the 'Cambrian explosion' of biodiversity (Zhuravlev & Riding, 2000; Zhuravlev & Wood 2008). Furthermore, it has recently been demonstrated that the Ediacaran group Palaeopascichnida had an agglutinated skeleton (Kolesnikov *et al.* 2018*a*, *b*).

Palaeopascichnida represents a problematic group of macroscopic fossils, which are globally distributed and can be numerically abundant in Ediacaran sequences (Fig. 1). They occur across the entire East European Platform (Finnmark, SE slope of the Baltic Shield, SE White Sea area, Moscow and Mezen basins, Central and South Urals, Podolia), as well as in South China, Avalonia (Newfoundland; Wales), Australia (Adelaide Rift Complex) and Siberia (Olenek Uplift, Uchur-Maya region) (Glaessner, 1969; Palij, 1976; Fedonkin, 1981, 1985; Cope, 1982; Narbonne *et al.* 1987; Becker & Kishka, 1989; Haines, 2000; Grazhdankin *et al.* 2008; Becker, 2010, 2013; Yuan *et al.* 2011; Högström *et al.* 2013; Grazhdankin, 2014; Kolesnikov *et al.* 2015; Nagovitsin *et al.* 2015; McIlroy & Brasier, 2016; Ivantsov, 2017, 2018; Jensen *et al.* 2018; Kolesnikov *et al.* 2018*a*, *b*; Hawco *et al.* 2019; Kolesnikov, 2019; Desiatkin *et al.* 2021). The term 'Palaeopascichnida' comes from the genus name *Palaeopascichnus* Palij, which initially was described from the Ediacaran deposits cropping out in Podolia, Ukraine (Palij, 1976). This taxon has previously been interpreted as trace fossils (Glaessner, 1969; Palij, 1976; Palij *et al.* 1979; Fedonkin, 1981; Becker, 2010, 2013; Parcha & Pandey, 2011), macrophytes (Haines, 2000), stratiform stromatolites (Runnegar, 1995) or rhizarians of foraminiferal affinity (Seilacher *et al.* 2003, 2005; Antcliffe *et al.* 2011; Seilacher & Mrinjek, 2011). Indeed, if we look at the exterior shape of fossils, a vague similarity can be seen between palaeopascichnids (Fig. 2a, c, e) and recent xenophyophore *Stannophyllum zonarium* (Fig. 2b), macrophyte *Padina pavonica* (Fig. 2d) and foraminifera *Morulaeplecta bulbosa* (Fig. 2f). Gehling & Droser (2009) proposed an alternative interpretation and regarded Palaeopascichnida as encrusting benthic organisms, comparing it to other so-called 'textured organic surfaces'. Recently, it has been demonstrated that *Palaeopascichnus linearis* represents the oldest known macroscopic organism with an agglutinated test, which has close affinity with modern xenophyophore organisms such

CAMBRIDGE UNIVERSITY PRESS

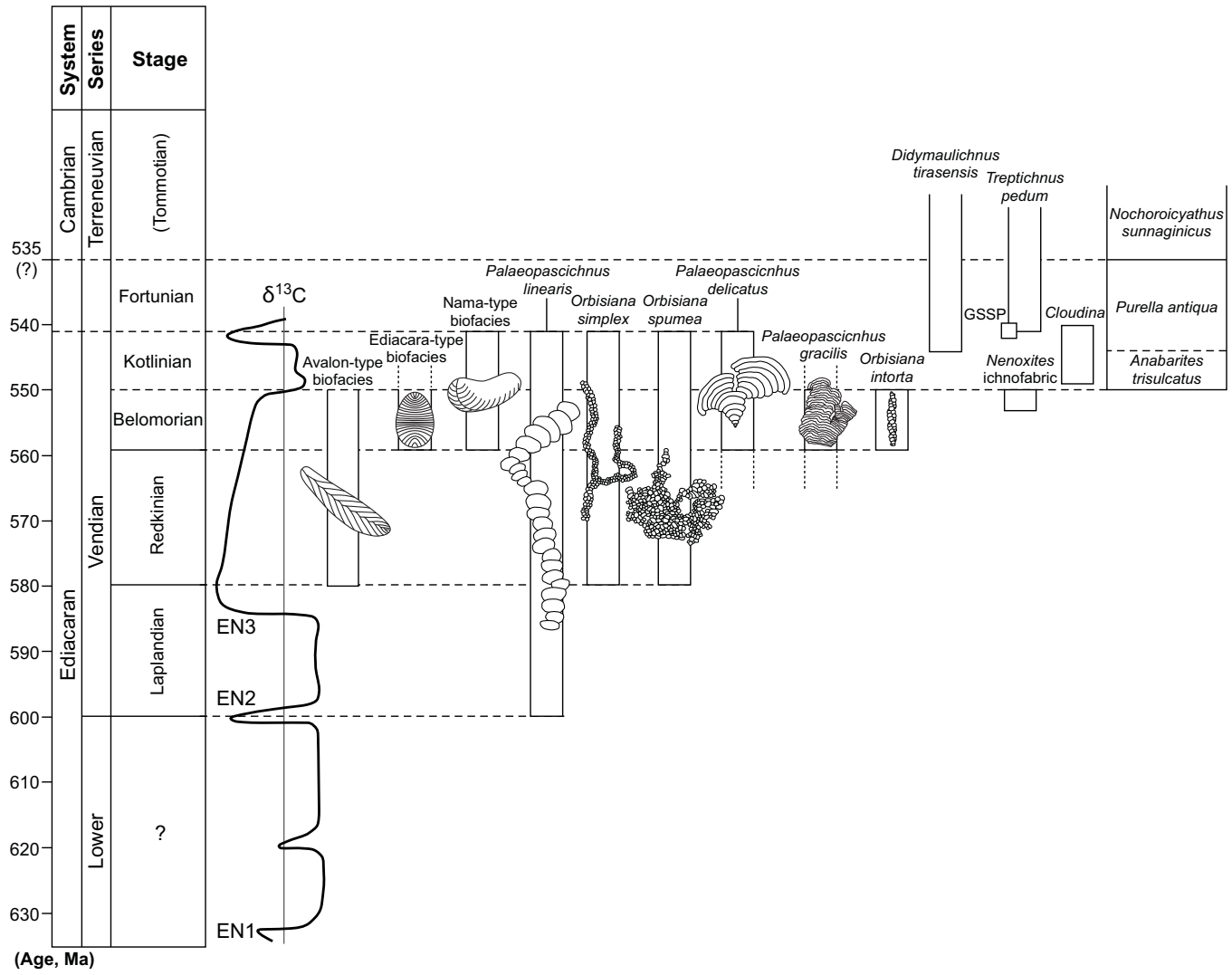

Fig. 1. Chronostratigraphic distribution of palaeopascichnids in the Ediacaran and the room for the 'Vendian Series' in the Standard Global Chronostratigraphic Chart (modified after Grazhdankin & Maslov, 2015).

as *Aschemonella monile* or *Psammina zonaria* (Kolesnikov *et al.* 2018*a*). Crucially, the understanding of palaeopascichnid morphology has advanced significantly since Hawco *et al.* (2019) proposed the combination of a morphometric and multivariate statistical approach using principal component analysis (PCA), which made it possible to recognize natural groups within the dataset of well-preserved fossil material from Newfoundland. For the moment, Palaeopascichnida includes several taxa and morphotypes, such as *Palaeopascichnus delicatus*, *P. linearis*, *P. gracilis* (new combination for *Yelovichnus gracilis* Fedonkin), *Orbisiana simplex* and foam- and spiral-like orbisianamorph multichambered structures (Kolesnikov, 2019), that are in need of revision and systematic description.

In this study we present a quantitative morphometric analysis of palaeopascichnid fossils from all known localities worldwide following the PCA method proposed by Hawco *et al.* (2019). On the one hand, we have simplified the parameter set (see Section 2); on the other hand the dataset has been expanded to comprise more than 1200 specimens of Palaeopascichnida, and sedimentary environments data have been added. The morphometric parameters and the fossil distribution are then tested with multivariate statistical approaches that allow us to discriminate species in genus *Palaeopascichnus*, and demonstrate palaeoenvironmental distribution and taxonomic diversification of both genera *Palaeopascichnus* (Fig. 3) and *Orbisiana* (Fig. 4). We also provide a revision of *Palaeopascichnus* and *Orbisiana* with description of new species.

2. Material and methods

This study is based on our examination of fossil material from the East European and Siberian platforms (881 specimens) and published photographic documentation from other areas (340 specimens), resulting in a dataset of 1221 specimens of Palaeopascichnida worldwide. Personally observed specimens of palaeopascichnid fossils were collected from outcrops and closely localized float of the Khatyspyt Formation in the Olenek Uplift of NE Siberia, Studenitsa and Mogilev formations of the Transdniester Podolia of Ukraine, Verkhovka and Lyamtsa formations of the SE White Sea area, Perevalok and Chernyi Kamen formations of the Central Urals and Basa Formation of the South Urals. An additional material of 84 specimens of Palaeopascichnida comes from the drill-hole cores of the Shotkusa-1, Dorogobuzh, Kepina-775, Soligalich-7 and Kotlas boreholes from northwest, north and northeast areas of

https://doi.org/10.1017/S0016756822000437 Published online by Cambridge University Press

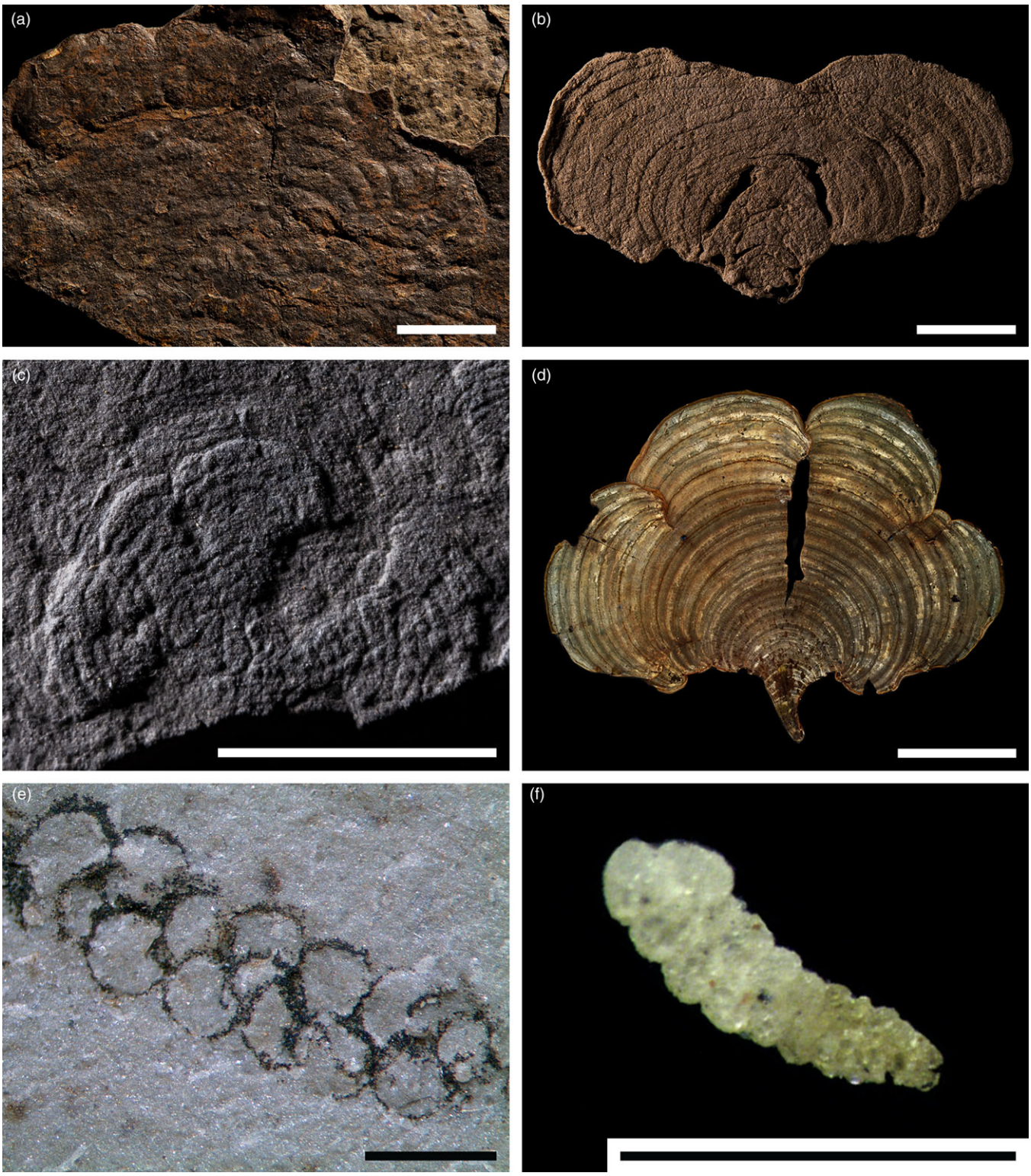

Fig. 2. Exterior similarity between fossil palaeopascichnids and recent organisms: (a) *Palaeopascichnus delicatus*, specimen M246/7014 (UGM, Yekaterinburg), Basa Formation, Asha Group, South Urals, Russia; (b) multichambered xenophyophore *Stannophyllum zonarium* (NHM, Copenhagen), from seamount in the central West Pacific; (c) *P. delicatus*, specimen 4716/9110 (PIN RAS, Moscow), Verkhovka Formation, Valdai Group, Onega Peninsula, White Sea area, Russia; (d) brown algae *Padina pavonica*, littoral zone in the central East Pacific; (e) *Orbisiana simplex*, Shotkusa-1 borehole (IPGG, St Petersburg), depth 225.7–218.5 m, Staraya Russa Formation, Redkino Group, Ladoga Basin, Russia; (f) benthic foraminifera *Morulaeplecta bulbosa*, North Sea area, midway between Denmark, Norway and Sweden (from Alve & Goldstein, 2010). Scale bars = 1 mm (black) and 10 mm (white).

https://doi.org/10.1017/S0016756822000437 Published online by Cambridge University Press

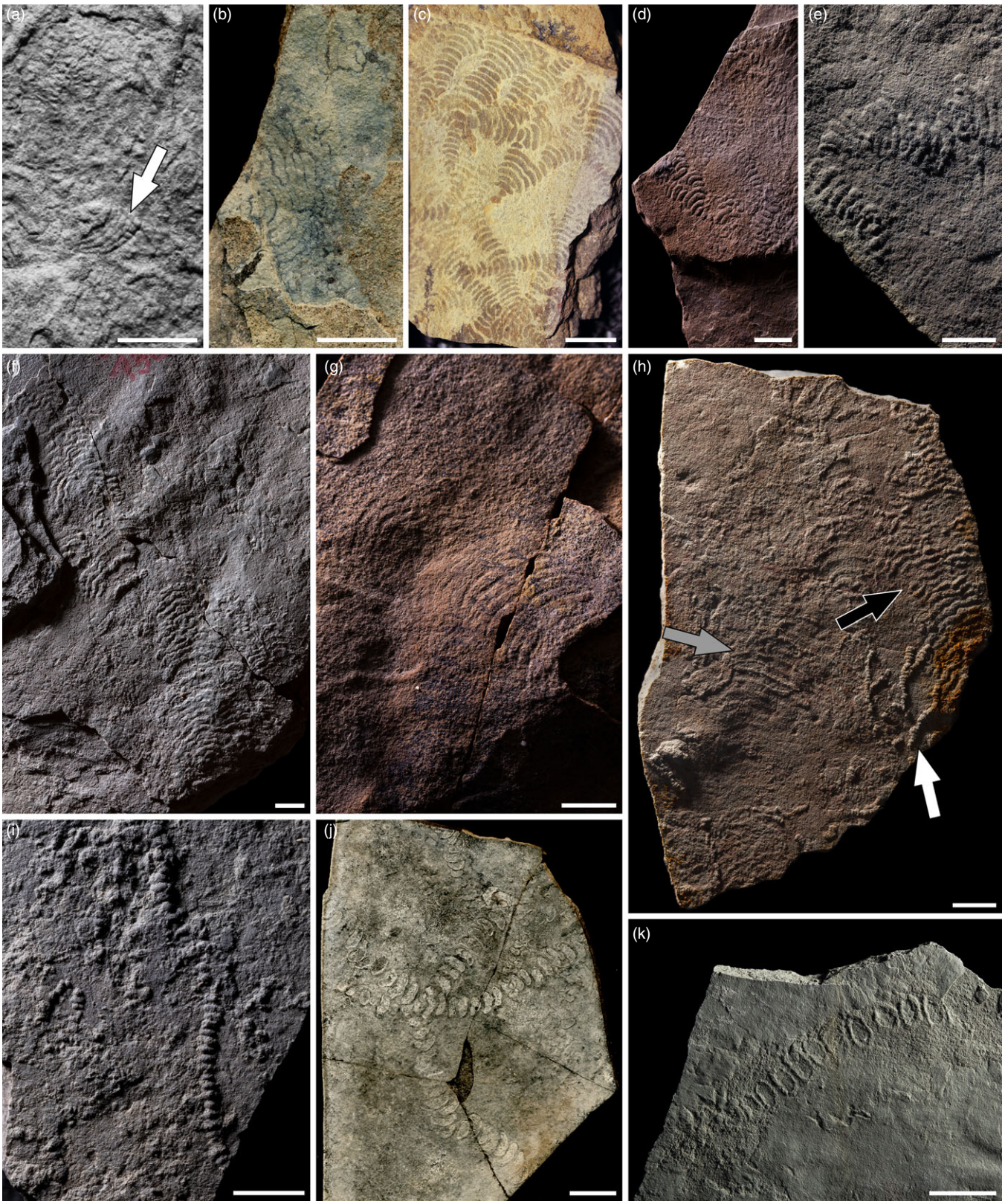

Fig. 3. Examples of morphological diversity in *Palaeopascichnus*: (a) *P. delicatus*, holotype (white arrow), specimen 1907/07 (NMNH NASU, Kiev), Komarovo beds, Kanilovka Group, Middle Dniester area, Ukraine (from Ivantsov *et al.* 2015); (b) *P. delicatus* (IPGG SB RAS, Novosibirsk), Pilipovo beds, Kanilovka Group, Middle Dniester area, Ukraine; (c) *P. delicatus*, specimen P36855 (SAM, Adelaide), Wonoka Formation, Adelaide Basin, South Australia; (d) *P. delicatus*, specimen CU20/1-24 (GIN RAS, Moscow), Chernyi Kamen Formation, Sylvitsa Group, Kosva River area, Central Urals, Russia; (e) *P. delicatus*, Khatyspyt Formation, Khorbusuonka Group, Olenek Uplift of Northeast Siberia, Russia; (f) *P. gracilis* comb. nov., holotype, specimen 3993/1309 (PIN RAS, Moscow), Verkhovka Formation, Valdai Group, Winter Coast of the White Sea area, Russia; (g) *P. gracilis* comb. nov., specimen CU20/2-4 (GIN RAS, Moscow), occurrence as in (d); (h) *P. delicatus* (grey arrow), *P. gracilis* (black arrow) and *P. linearis* (white arrow) preserved on the same bedding plane, as in (f); (i) *P. linearis*, specimen 3392/3153 (PIN RAS, Moscow), Verkhovka Formation, Valdai Group, Syuzma River, Onega Peninsula, White Sea area; (j) *P. linearis,* occurrence as in (e); (k) *P. linearis,* specimen CSGM WC/2018-3 (IPGG SB RAS, Novosibirsk), occurrence as in (f). Scale bars = 10 mm.

https://doi.org/10.1017/S0016756822000437 Published online by Cambridge University Press

Fig. 4. Fossils of genus *Orbisiana*: (a) *O. simplex*, holotype, specimen CSGM 2076-001 (IPGG SB RAS, Novosibirsk), Soligalich-7 borehole, depth 2060–2025 m, Nelidovo beds, Gavrilov Yam Formation, Redkino Group, Moscow Basin, Russia; (b, c) *O. simplex*, Shotkusa-1 borehole (IPGG RAS, St Petersburg), depth 225.7–218.5 m, Staraya Russa Formation, Redkino Group, Ladoga Basin, Russia; (d) *O. simplex*, specimen CSGM 2079-80 (IPGG SB RAS, Novosibirsk), Verkhovka Formation, Valdai Group, Syuzma River, Onega Peninsula, White Sea area; (e) *O. spumea* sp. nov. (white arrow), specimen 4853/1586 (PIN RAS, Moscow), and scratch marks of *Kimberella* sp. on the same bedding plane, Verkhovka Formation, Valdai Group, Winter Coast of the White Sea area, Russia; (f) *O. spumea* sp. nov., holotype, specimen CSGM 2079-80 (IPGG SB RAS, Novosibirsk), occurrence as in (d); (g) pyritized *O. spumea* sp. nov., occurrence as in (b); (h) *O. intorta* sp. nov., holotype, specimen CSGM 2079-29 (IPGG SB RAS, Novosibirsk), occurrence as in (d); (i) *O. intorta* sp. nov., occurrence as in (e); (j, k) *O. intorta,* sp. nov. (white arrow) preserved on erosional surface of concentric scratch circles (swing marks), occurrence as in (D). Scale bars = 1 mm (black) and 10 mm (white).

the East European Platform. Other specimens of palaeopascichnid-like fossils were incorporated into our dataset using published photographs from Newfoundland (Narbonne *et al.* 1987; Gehling *et al.* 2000; Liu & McIlroy 2015; Hawco *et al.* 2019), Wales (Cope, 1982; Liu & McIlroy, 2015), Norway (McIlroy & Brasier, 2016; Jensen *et al.* 2018), the Transdniester Podolia of Ukraine (Palij, 1976; Palij *et al.* 1979; Fedonkin, 1983, 1985, 1990; Martyshin, 2012), the Arkhangelsk region of Russia (Chistyakov *et al.* 1984), the Uchur-Maya Basin of Eastern

https://doi.org/10.1017/S0016756822000437 Published online by Cambridge University Press

Siberia (Ivantsov, 2017), Australia (Glaessner, 1969; Jenkins, 1995; Haines, 2000; Gehling *et al.* 2005; Gehling & Droser, 2009), South China (Wan *et al.* 2014) and India (Parcha & Pandey, 2011).

The studied specimens are well preserved, with clear edges in various sedimentary rocks as epi- and hypo-relief fossils. The specimens are characterized by differences in shape and size of chambers and in the degree of growth, elongation and expansion along the series or aggregate clusters. In order to develop the quantitative and statistical discrimination of morphospecies within the genus *Palaeopascichnus* we follow the PCA method that has recently been tested on similar fossil material from Newfoundland (Hawco *et al.* 2019). Compared to that study, measures are limited to chamber width and minimum and maximum chamber length (Fig. 5). On the one hand, this allowed us to simplify and speed up the measuring process, but on the other hand, we have expanded statistical analysis to all known fossil localities. From the direct measurements other morphological parameters were calculated, such as minimum/maximum length to minimum/maximum width ratios. These parametric ratios were chosen because they focus on chamber shape and its morphological variability within the *Palaeopascichnus*. Assuming that branched *Palaeopascichnus* was probably a single, continuous structure (Hawco *et al.* 2019), we also consider branching specimens as single organisms. *Orbisiana* is generally a palaeopascichnid organism, but differs dramatically in the number of chambers, and the constant globular shape of chambers, forming multiserial regular or biserial spiral-like structures and foam-like irregular aggregates (Kolesnikov *et al.* 2018*b*; Kolesnikov, 2019). For the multivariate statistical analysis we have included *Palaeopascichnus*-like organisms only, which are characterized by a single, occasionally branching, series of chambers. In the interest of a pilot study abundance, density, similarity and difference in ecological and taxonomic diversification of both genera, the dataset has been expanded by adding sedimentary environments data from personal observations and publications. Thus, the dataset includes information on 1034 specimens of *Palaeopascichnus* and 187 of *Orbisiana*.

The studied material (Figs 2–4) was imaged using a Canon EOS 6D Mark II digital single-lens reflex camera with a Canon EF 100 mm f/2.8 Macro IS USM lens mounted on a Canon Extension Tube (EF 25 II); Fujifilm GFX 50r digital mirrorless medium format camera with a Fujinon GF 120 mm f/4.0 R LM OIS Macro lens mounted on a Fujifilm Macro Extension Tube (MCEX-45G WR); and Epson Perfection V600 Photo digital scanner. All analyses were run using the programming language R, version 4.0.3 (R Core Team 2020), and integrated development environment RStudio, version 1.4.1103 (RStudio, PBC 2021). PCA is used in this study on morphological parameters, with the goal of reducing dimensionality in a multivariate dataset. The principal components are linear combinations of the variables, and which compose for the predominance of variation in the specimens (Dillon & Goldstein, 1984). For the purpose of identifying which of the parameters control the coordinates of the PCA space, here we used the 'FactoMineR' package for the RStudio (F Husson *et al.*, unpub. technical report, 2010) that allowed us to explore the degree to which each parameter has contributed to the construction of each numerical dimension (by using the dimdesc output). Hawco *et al.* (2019) carried out the PCA on various iterations for two parameter sets used singularly and together (i.e. shape parameters only; size parameters only; and both shape and size). As a result, they have demonstrated that the studied *Palaeopascichnus* specimens split into three statistically identified clusters and represent different morphotypes independently on chosen parametric iterations. In our study, several iterations were carried out for the two parameter sets used singularly and combined (such as width ratio only; chamber elongation ratio; and both width and chamber elongation ratios). This allowed us to better understand which of the measured morphological features has the most impact on the clustering of specimens in the dataset.

To determine natural groups (morphotypes or morphospecies) within the dataset of 1034 specimens of *Palaeopascichnus* we performed hierarchical clustering on principal components (HCPC) on the PCA results. This is recognized to be one of the best and easiest methods for determining natural groupings (Dillon & Goldstein, 1984). The number of clusters in our dataset is defined through inertia gain analysis being a variation measure of the within-group variance plotted as a histogram of variance versus number of clusters (Fig. 6). The biggest jumps in inertia gain are taken as nodes at which it is possible to divide the obtained dendrogram into clusters (F Husson *et al.*, unpub. technical report, 2010 Hawco *et al.* 2019). This results in an updated dataset as separate clusters containing all previously measured morphological parameters and sedimentary environments data.

As the only characters we used in PCA are parametric ratios, it can be surmised that these are susceptible to overprinting by tectonic strain. While specimens from a locality with minimal tectonic overprint and deformation can be assumed to have been very little altered from their original shapes, it is clear that the same cannot be assumed when comparing specimens of palaeopascichnids from terranes with very different diagenetic and metamorphic history and, in most cases, it may not be possible to retrodeform specimens studied only from published photographs. However, in this study most specimens of *Palaeopascichnus* were examined from original fossil material, where the large majority of palaeopascichnid specimens are preserved in fine-grained sedimentary rock without any visible tectonic deformation or metamorphic changes. In order to check this, we have done PCA tests for the entire dataset and separately for different fossil localities in the Central Urals, the Olenek Uplift of Siberia and Newfoundland.

An important statistical tool in modern ecology is the regression analysis provided by generalized linear models (GLMs) and generalized additive models (GAMs) (Guisan *et al.* 2002). In defining the ecological diversification of extinct Palaeopascichnida, statistical models are no exception and are one of the essential tools in the field of Ediacaran palaeoecology. GLMs are a mathematical extension of linear models that do not force numeric data into an unnatural scale, and thus allow for non-linearity and non-constant variance structure in the dataset, whereas GAMs are a semi-parametric extension of GLMs, where the mathematical functions are additive and the components are smooth (Hastie & Tibshirani, 1986). In addition, both linear and nonlinear models may be constructed by the sum of smooth functions of predictor variables (parameters), in which it is common to use polynomial intervals also known as 'splines' (Wood, 2006). These have often been used to explore the relationship and interactions between environmental variables (i.e. sedimentary environments or depositional settings) and the presence of a species given isolated or worldwide localities (Murase *et al.* 2009). Thus, using both GAMs and GLMs enables the best representation of the dataset to be identified and selected.

In this study, the effectiveness of linear and nonlinear generalized models to identify the effect of sedimentary environment variables on the abundance of the six species of the Palaeopascichnida (1221 specimens) from different fossil localities worldwide was

https://doi.org/10.1017/S0016756822000437 Published online by Cambridge University Press

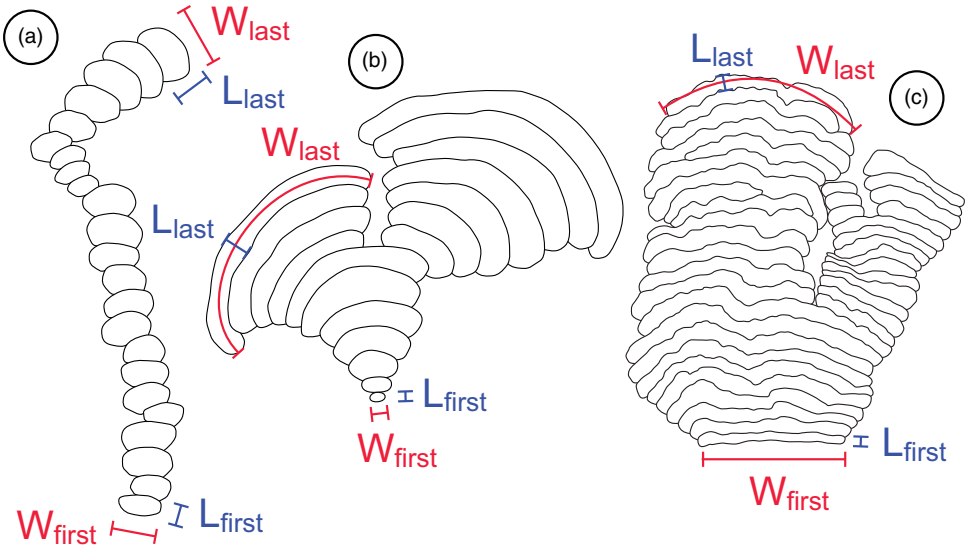

Fig. 5. Schematic representations of *Palaeopascichnus*: (a) organism has chambers arranged in series, with narrow width of chambers and shape being little variable; (b) specimen showing chambers arranged in series, with chamber shape being highly variable from globular to highly elongated throughout the series; (c) organism has chambers arranged in series, with highly elongated chambers, but chamber shape showing little variation.

examined (Fig. 7). Sedimentary environment data were involved in our dataset as the numeric values of definite depositional settings of the fossil material, based on personal observations on the East European and Siberian platforms and respective publications (see Table S1 in the Supplementary Material available online at https://doi.org/10.1017/S0016756822000437). Relying on the experience and knowledge of previous scholars, we did not provide quality control on the data used from published materials and interpretations of depositional settings palaeopascichnid-hosted sedimentary rocks. Based on depositional environment, ten values ranging from extremely shallow continental (value 1) to relatively deep carbonate facies (value 10) were defined. We treated these values as nominal, which allowed us to simplify the dataset and use numeric values for statistical analysis. GLMs are included in standard R and RStudio packages. Available models are linear, exponential and cubic (polynom degrees are 1, 2 and 3 respectively), as higher-degree polynomial models would result in more than the unimodal shape of the plotted curve. Selection of the model was done both manually and automatically, based on the AIC test criterion, allowing us to select the model with the lowest deviance of analysed data. GAMs are included in the R and RStudio packages. The models with a fixed degree of freedom (polynom degrees are 3, 4 and 5 respectively) are available and automatic selection was done based on the AIC test criterion. The palaeoenvironmental optimum is simply the value of the parametrical gradient, in which the *Palaeopascichnus* and *Orbisiana* species have the highest probability of occurrence in depositional settings based on the particular model. In the context of identifying which of the parameters define the environmental optimum, we used the 'vegan' and 'mgcv' packages for the RStudio (Oksaken *et al.* 2020). The optimum of Palaeopascichnida is identical with the highest value of the species abundance gradient, if the response curve shows more-or-less monotone Gaussian-like distribution; the tolerance range is determined as part of the gradient, where the predicted probability of species abundance is higher than 80 % of the maximum value for predicted probability (Mastitsky & Shitikov, 2015). From this the palaeoenvironmental distribution of the Ediacaran genera *Palaeopascichnus* and *Orbisiana* can be calculated (Fig. 7). However, bearing in mind their global distribution and unpublished/missing data, our database of 1221 specimens is obviously incomplete.

3. Results

Orbisiana is composed of globular chambers that are organized into multiserial chain- or grape-like aggregates (Fig. 4a–d), irregular foam-like clusters (Fig. 4e–g) and regular biserial spiral- or fusiform structures (Fig. 4h–k). The chamber varies between 0.25 mm and 2 mm in diameter. The shape of the chambers is globular and relatively consistent within an aggregate or irregular cluster. Although it shares the chambered construction with *Palaeopascichnus*, the *Orbisiana* differs markedly and has multiserial or irregular arrangement of the chambers, and for that reason they were not included into the dataset for PCA test. For the moment, *Orbisiana simplex* (Fig. 4a–d) was the only valid and described taxon within the genus (Kolesnikov *et al.* 2018*b*). Drawing on the difference in the chamber arrangement and the absence of observed transitional morphotypes, the introduction of two new species is suggested: *Orbisiana spumea*, an irregular foam-like multichambered structure (Fig. 4e–g), and *Orbisiana intorta*, with a biserial fusiform multichambered test (Fig. 4h–k).

Palaeopascichnus is composed of chambers that are organized into single chain-like series, elongated and occasionally branching structures (Fig. 3). The series consist of globular or allantoid chambers 1–40 mm in width. Chambers are relatively consistent in size within a series (e.g. Fig. 3f, i) or significantly increase in width successively (Fig. 3a–e). Comparison of the three iterations (such as width ratio only, chamber elongation ratio only, and both ratios) demonstrates similarity in the clustering plots of the PCA tests, where these variables are correlated to both axes. Results of the four PCA tests for all known fossils of *Palaeopascichnus* (Fig. 6a), 356 specimens from the Khatyspyt Formation in the Olenek Uplift of Siberia (Fig. 6b), 96 specimens from the Chernyi Kamen Formation in the Central Urals (Fig. 6c), and for the 108 specimens from the Fermeuse Formation, Newfoundland (Fig. 6d), are displayed separately. These were calculated and plotted on the third iteration (width ratio W_{last}/W_{first} and chamber elongation ratio W_{last}/L_{last}). For all parameters in that iteration the first dimension (Dim1) accounts for *c.* 57–63 % of the total variance, and the second dimension (Dim2) *c.* 33–40 %. The inertia gain supports a division into three clusters for the global *Palaeopascichnus* dataset (Fig. 6a), Olenek Uplift (Fig. 6b), Central Urals (Fig. 6c), and for Newfoundland separately (Fig. 6b). These three clusters show a

https://doi.org/10.1017/S0016756822000437 Published online by Cambridge University Press

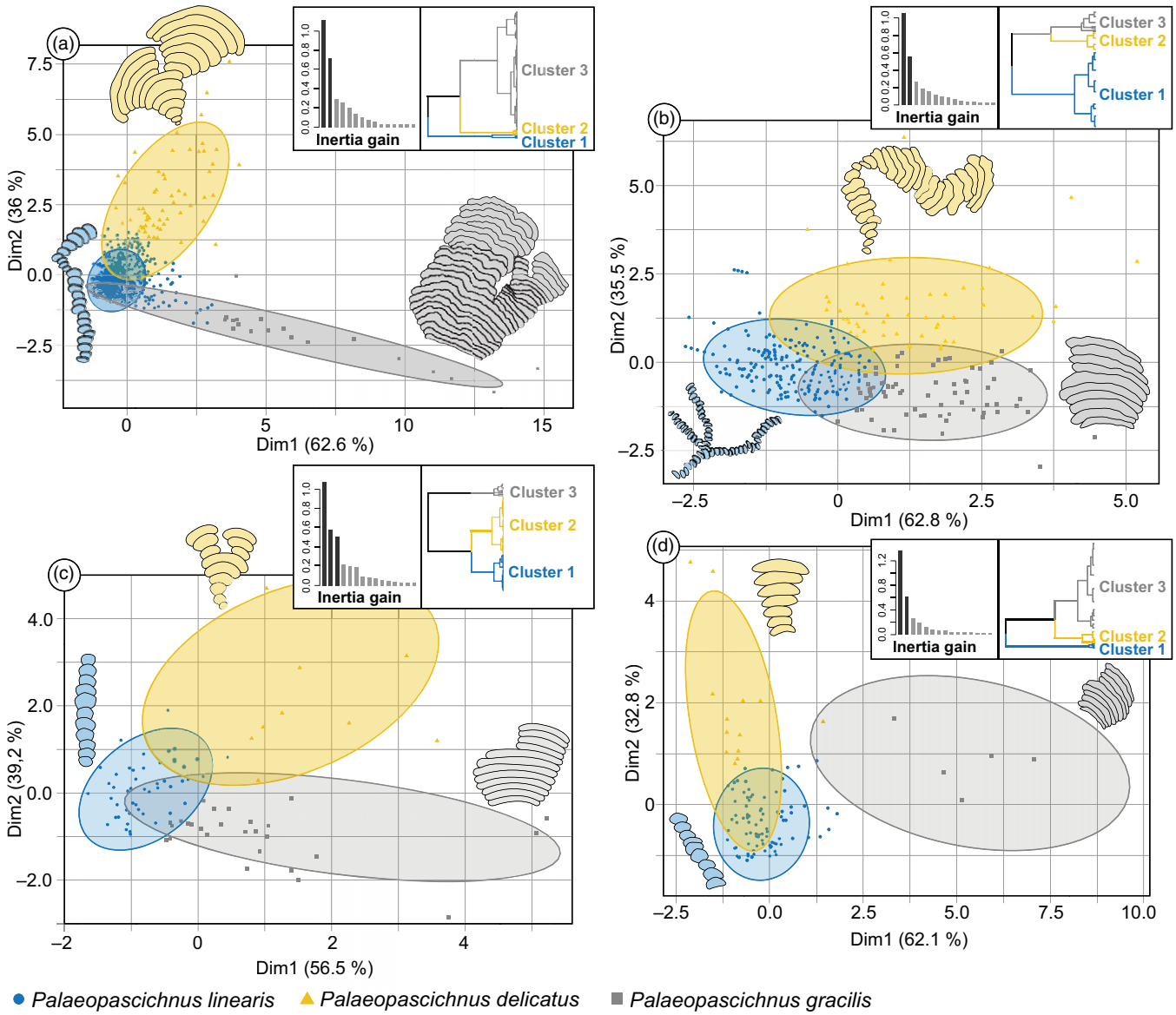

Fig. 6. Results of principal component analysis (PCA) and hierarchical clustering on principal components (HCPC) tests on the global dataset of *Palaeopascichnus* specimens (a), including all individuals for which shape and length/width parameters could be determined (number of specimens = 1034); (b) specimens from the Upper Vendian Khatyspyt Formation, Khorbusuonka Group, Olenek Uplift of Siberia (number of specimens = 356); (c), specimens from the Upper Vendian Chernyi Kamen Formation, Sylvitsa Group, Central Urals, Russia, observed on one bedding plane, *c.* 1.5 m^2 (number of specimens = 96); and (d) specimens from the Ediacaran Fermeuse Formation, St John's Group, Newfoundland (number of specimens = 108). All PCA plots display three separate clusters as different morphotaxa. Inertia gain supports division into three clusters. HCPC plot shows hierarchical separation of the measured specimens into three clusters.

partial overlap but also occupy distinct distribution areas in the PCA space.

In the entire dataset (Fig. 6a), cluster 1 consists of 957 specimens that are characterized by a relatively consistent size and shape of chambers throughout the series. The width ratio (W_{last}/W_{first}) is relatively constant at 1.25–1.5. The chamber elongation ratio (W_{last}/L_{last}) does not exceed 2.5–2.6 and mainly ranges between 1 and 1.5. Previously redescribed *Palaeopascichnus linearis* (Kolesnikov *et al.* 2018*a*) fits the main area of this cluster in the PCA space. Cluster 2 consists of 58 specimens that are typified by a progressively increasing chamber width, and the last chamber can be several (up to 10–20) times wider than the initial one. Assuming palaeopascichnida are protozoan organisms (Seilacher *et al.* 2003; Kolesnikov *et al.* 2018*a*, *b*; Hawco *et al.* 2019), growth can be simplified as the increase in cytoplasm and organelles of a cell through time. Thus, chamber shape varies from smaller globular in the initial chamber to bigger allantoid or extremely elongated sausage- and arc-like in the last one. The type species *Palaeopascichnus delicatus* (Palij, 1976) fits the gross area of cluster 2 in the PCA space. Cluster 3 consists of 19 specimens distinguished by significantly wider chambers than the overall total mean. The width ratio is relatively constant as in cluster 1, but the shape is extremely elongated throughout the series. Also worth noting is that the chamber width can insignificantly both increase and decrease along the series. The species *Palaeopascichnus gracilis*, which was initially described as *Yelovichnus gracilis* (Fedonkin, 1985) from the White Sea area, fits the main part of the cluster 3 area. Thus, the 1034 specimens of *Palaeopascichnus* fossils processed in this study show a sufficient range of chamber shapes (width or elongation ratios) to consider three separate morphometric clusters as different species.

https://doi.org/10.1017/S0016756822000437 Published online by Cambridge University Press

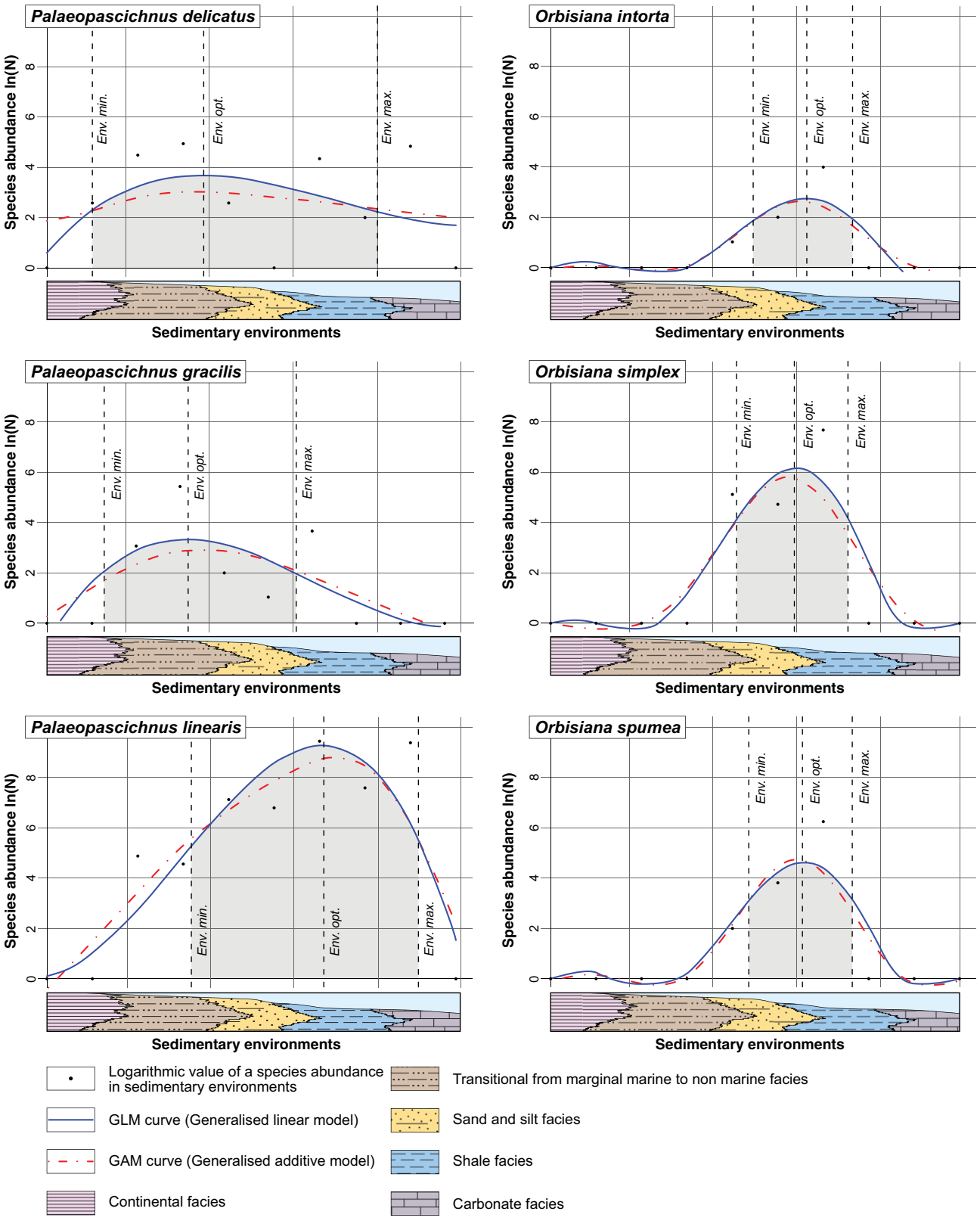

Fig. 7. Results of study of palaeoenvironmental distribution of *Palaeopascichnus* and *Orbisiana* on the dataset of specimens worldwide (number of specimens = 1034). Generalized linear (GLM) and additive (GAM) model curves almost coincide. *Palaeopascichnus* demonstrates variable palaeoenvironmental distribution; *Orbisiana* shows essentially identical distribution of the three species and narrower diversity range.

https://doi.org/10.1017/S0016756822000437 Published online by Cambridge University Press

The carbonate-hosted palaeopascichnids from the Olenek Uplift of Siberia are preserved in intervals of finely laminated limestones of the Khatyspyt Formation which was not affected by tectonic strain. In the Olenek Uplift (Fig. 6b), cluster 1 consists of 232 specimens that are also characterized by relatively consistent size and shape of chambers throughout the series. The width ratio is *c.* 1.75–2.0. The chamber elongation ratio does not exceed 1.75–2.0. *P. linearis* fits the area of this cluster in the PCA space. Cluster 2 consists of 53 specimens that are typified by a progressively increasing chamber width, and the last chamber can be up to six times wider than the initial one. The chamber shape varies from globular in the initial chamber to allantoid or crescent-like in the last one. *P. delicatus* fits the main area of cluster 2 in the PCA space. Cluster 3 consists of 71 specimens distinguished by wider chambers than in clusters 1 and 2. *P. gracilis* fits the main part of the cluster 3 area, and *P. linearis* fits some part in it. Despite all three clusters showing an insignificant overlap, they occupy clearly distinct areas in the PCA space.

The siliciclastic-hosted palaeopascichnids from the Central Urals are preserved in intervals of thinly laminated fine-grained silt- and sandstones of the Chernyi Kamen Formation which was affected by tectonic strain, being a part of the Urals Fold Belt. In the Central Urals (Fig. 6c), cluster 1 consists of 60 specimens characterized by relative consistency in the size and shape of chambers. The width ratio ranges from 1.0 to 1.5; the chamber elongation ratio does not exceed 1.75. *P. linearis* fits the area of this cluster in the PCA space. Cluster 2 consists of eight specimens that are typified by constantly increasing width of chambers (chamber elongation ratio reaches 5.5); the chamber shape changes from almost globular at the beginning to elongated and arched at the end of the series. *P. delicatus* fits the main area of cluster 2 in the PCA space. Cluster 3 consists of 28 specimens that are characterized by relatively constant size of chambers, but their shape is significantly elongated. *P. gracilis* fits the major part of the cluster 3 area. Clusters occupy distinct areas in the PCA space.

The palaeopascichnids from Newfoundland are preserved in fine-grained silt- and sandstones of the Fermeuse Formation which might be affected by tectonic strain. Measurements in 90 specimens were taken from Hawco *et al.* (2019); 28 specimens were collected personally by A. Kolesnikov during field work in 2015. In Newfoundland (Fig. 6d), cluster 1 consists of 90 specimens that are characterized by a relatively consistent size and shape of chambers throughout the series. The width ratio varies in the range 1.1–2.1. The chamber elongation ratio mainly ranges between 1.5 and 2.5. *P. linearis* fits the main area of cluster 1 in the PCA spaces, although it partially overlaps with cluster 2. Cluster 2 consists of 13 specimens typified by a progressively increasing chamber width, and the last chamber can be up to five times wider than the initial one; the chamber shape varies from slightly elongated in the initial chamber to allantoid in the last one. *P. delicatus* fits the main area of cluster 2 in the PCA space. Cluster 3 consists of five specimens characterized by relatively constant size of chambers (width ratio is 1.17–2.14) and significantly elongated shape (chamber elongation is 7.5–9.0). *P. gracilis* fits the entire part of the cluster 3 area. As in the global dataset, the Central Urals and the Olenek Uplift, the clusters in Newfoundland occupy distinct areas in the PCA space. Therefore, taphonomy and preservation styles have not significantly affected discrimination of morphotaxa within the genus *Palaeopascichnus*.

The results of the palaeoenvironmental distribution analysis display a good linear relationship (GLM) between the abundance of orbisianids and the sedimentary environments predictor value (Fig. 7). The orbisianid diversity variance explained by the linear models was 74.6 % for *Orbisiana intorta*, 77.9 % for *Orbisiana simplex* and 82.7 % for *Orbisiana spumea*, closely matching the percentages explained by the GAMs. When referring to statistical significance, a value of 90 % confidence (i.e. $p < 0.1$) and remarkably lower square mean error value in both models were used throughout. As a result, both GLM and GAM demonstrate a relatively narrow palaeoenvironmental tolerance ranging in between sand/silt and shale facies, with an optimum in shale for all *Orbisiana* species (Fig. 7). All *Orbisiana* species demonstrate an identical palaeoenvironmental optimum in shale facies and a relatively narrow tolerance range, unlike the situation within *Palaeopascichnus* species.

The *Palaeopascichnus* distribution also shows a good linear relationship between the fossil abundance and the environmental predictor (Fig. 7). The *Palaeopascichnus* diversity variance explained by the linear models was 45.9 % for *Palaeopascichnus delicatus*, 48.8 % for *Palaeopascichnus gracilis* and 82.5 % for *Palaeopascichnus linearis*, which are similar to the percentages explained by the GAMs (a value of 83 % confidence, i.e. $p < 0.17$). The GLM and GAM display palaeoenvironmental optimum and tolerance range in the sedimentary environments (Fig. 7). *Palaeopascichnus delicatus* has the widest tolerance range, from continental facies of extremely shallow sedimentary environment (Bobkov *et al.* 2019; Sozonov *et al.* 2019; Desiatkin *et al.* 2021) to carbonate facies of deeper depositional settings (Grazhdankin *et al.* 2008; Nagovitsin *et al.* 2015; Mitchell *et al.* 2020), with a palaeoenvironmental optimum in between non-marine and marine facies. *Palaeopascichnus gracilis* shares its palaeoenvironmental optimum with *P. delicatus*, except for a shift to shallower settings and environmental maximum limited to shale facies. *Palaeopascichnus linearis* shows a palaeoenvironmental optimum in the relatively deeper shale facies, and its tolerance range is limited in between shallow marine and carbonate facies.

In summary, we have a sufficient number of different characters, including morphological features and statistical data, to allow us to discriminate not only between *Palaeopascichnus* and *Orbisiana* but also the species within them. This allows us to advance our understanding of the systematic palaeontology and revision of the group Palaeopascichnida worldwide (Table S1 in the Supplementary Material available online at https://doi.org/10.1017/S0016756822000437).

4. Systematic palaeontology

Genus *Orbisiana* Sokolov, 1976

1976 *Orbisiana* Sokolov, p. 138, text-fig.

2018 *Orbisiana* Kolesnikov *et al.* pp. 202–3.

Type species. Orbisiana simplex Sokolov, 1976

Emended diagnosis. Compact elongate fusiform structures or grape-like clusters and irregular aggregates of globular chambers (0.25–2 mm in diameter). Chamber size tends to be uniform within each cluster or aggregate but varies among individuals.

Species composition. Orbisiana simplex, *O. intorta* and *O. spumea*.

Remarks. Kolesnikov *et al.* (2018*b*) reassessed the type material of *Orbisiana simplex* Sokolov from the Moscow Basin and coeval material from the White Sea area. It was shown that the species *Orbisiana simplex* has multichambered construction in the shape of elongate grape-like clusters. However, Seilacher *et al.* (2003) reported that globular chambers may be arranged into spiral and foam-like structures. A new abundant fossil material from

https://doi.org/10.1017/S0016756822000437 Published online by Cambridge University Press

the White Sea area, the South Urals and numerous drill-cores from the East European Platform confirms this. It was therefore suggested that the diagnosis of *Orbisiana* be revised taking into consideration the new data on its morphology.

Orbisiana simplex Sokolov (1976) (Figs 2e, 4a–d)

For earlier synonymy see Kolesnikov *et al.* (2018*b*).

2018 *Orbisiana simplex* Kolesnikov *et al.* pp. 199–201, figs 2a–j, 3a, 4a–c.

2018 'orbisianid development' Jensen *et al.* (2018), p. 5, fig. 3c (*partim*).

2019 *Orbisiana simplex* Kolesnikov, p. 3, fig. 1d.

Holotype. Specimen No. CSGM 2076-001 (Fig. 4a) stored in the Center of Palaeontological, Micropalaeontological and Palynological Collections 'GEOKHRON' of the Trofimuk Institute of Petroleum Geology and Geophysics, Novosibirsk, Russia.

Type locality. Soligalich-7 borehole (depths 2153–2114 m) drilled *c.* 10–15 km from the town of Soligalich, Kostroma region, Russia; middle part of the Lower Member of the Gavrilov Yam Formation (*c.* 580–560 Ma).

Description. Globular chambers arranged in compact grape-like clusters and constituting sinuous linear aggregates, the longest measured at 70 mm and comprising over 150 chambers. The width of the aggregates varies between 0.5 and 5.0 mm. Aggregates can branch, with no appreciable change in chamber sizes or shape, into two branches that are similar in appearance.

Occurrence. (1) Soligalich-7 borehole (depths 2153–2114 m), Kostroma region, Russia; Lower Member, Gavrilov Yam Formation, Redkino Group, Upper Vendian, Ediacaran (Kolesnikov *et al.* 2018*b*). (2) Shotkusa-1 borehole (depths 225.7–218.5 m), Leningrad region, Russia; Staraya Russa Formation, Redkino Group, Upper Vendian, Ediacaran (Kushim *et al.* 2016; Golubkova *et al.* 2018). (3) Kunevichi-4 borehole (depth 557–558 m), Leningrad region, Russia; Staraya Russa Formation, Redkino Group, Upper Vendian, Ediacaran (Jensen, 2003). (4) Kepina-775 borehole, Arkhangelsk region, Russia; Lyamtsa Formation, Valdai Group, Upper Vendian, Ediacaran (pers. obs.). (5) Onega Peninsula, Lyamtsa River, Arkhangelsk region, Russia; Lyamtsa and Verkhovka formations, Valdai Group, Upper Vendian, Ediacaran (pers. obs.). (6) Onega Peninsula, Solza River, Arkhangelsk region, Russia; Verkhovka Formation, Valdai Group, Upper Vendian, Ediacaran (pers. obs.). (7) Onega Peninsula, Syuzma River, Arkhangelsk region, Russia; Verkhovka Formation, Valdai Group, Upper Vendian, Ediacaran (pers. obs.). (8) South Urals, Tramshak River, Republic of Bashkortostan, Russia; Basa Formation, Asha Group, Upper Vendian, Ediacaran (pers. obs.). (9) Transndniester Podolia, Khmelnitskyi region, Ukraine; Mogilev Formation, Mogilev–Podolsky Group, Upper Vendian, Ediacaran (*sensu* Fedonkin, 1983). (10) South Urals, Inzer River, Republic of Bashkortostan, Russia; Basa Formation, Asha Group, Upper Vendian, Ediacaran (Kolesnikov, 2019).

Material. 132 specimens.

Orbisiana intorta sp. nov. (Fig. 4h–k)

2019 'spiral-like orbisianamorph structure' Kolesnikov, p. 3, fig. 1f.

Etymology. From Latin '*intortus*' fusiformed, in reference to the spindle-like strombuliform structure.

Holotype. Specimen No. CSGM 2079-29 (Fig. 4h) stored in the Center of Palaeontological, Micropalaeontological and Palynological Collections 'GEOKHRON' of the Trofimuk Institute of Petroleum Geology and Geophysics, Novosibirsk, Russia.

Type locality. Approximately 5.7 km upstream of the mouth of Suzma River, Onega Peninsula, SE White Sea area, *c.* 80 km west of Arkhangelsk, NW Russia.

Diagnosis. Recumbent macroscopic organism consisting of globular, submillimetre- to millimetre-sized chambers, which are arranged into biserial linear or slightly curved non-branched fusiform- or spindle-like agglutinated test.

Occurrence. White Sea area, Onega Peninsula, Syuzma River, Arkhangelsk region, Russia; Verkhovka Formation, Valdai Group, Upper Vendian, Ediacaran (pers. obs.).

Material. Eight specimens.

Remarks. Orbisiana intorta is a new taxon represented by spindle-like strombuliform structures found in the Verkhovka Formation on the White Sea area only. This species demonstrates the absence of diverging. The type collection is represented by sinistrally coiled spindle-like structures, but dextrally coiled spindles from the same area are also known (Anton Legouta's unpublished data). The type collection is stored in the Trofimuk Institute of Petroleum Geology and Geophysics, Novosibirsk, Russia.

Orbisiana spumea sp. nov. (Fig. 4e–g)

1981 *Neonereites* Fedonkin, p. 78, pl. XIV, figs 3, 4 (*partim*).

1985 *Orbisiana* Gnilovskaya, p. 193, pl. XXXIII, fig. 7.

1990 *Orbisiana* Gnilovskaya, p. 279, pl. 33, fig. 7.

2018 *Neonereites multiserialis* Ivantsov *et al.* p. 185, pl. IX, fig. 1a, b.

2019 'foam-like orbisianamorph structure' Kolesnikov, p. 3, fig. 1e.

Etymology. From Latin '*spuma*' spumy, in reference to the flattened foam-like (or spumy-like) structure.

Holotype. Specimen No. CSGM 2079-48 (Fig. 4f) stored in the Center of Palaeontological, Micropalaeontological and Palynological Collections 'GEOKHRON' of the Trofimuk Institute of Petroleum Geology and Geophysics, Novosibirsk, Russia.

Type locality. Approximately 5.7 km upstream of the mouth of Suzma River, Onega Peninsula, SE White Sea area, *c.* 80 km west of Arkhangelsk, NW Russia.

Diagnosis. Recumbent macroscopic organism consisting of numerous globular submillimetre- to millimetre-sized chambers in a foam-like clustered array.

Occurrence. (1) Soligalich-7 borehole (depths 2153–2114 m), Kostroma region, Russia; Lower Member, Gavrilov Yam Formation, Redkino Group, Upper Vendian, Ediacaran (Kolesnikov *et al.* 2018*b*). (2) Shotkusa-1 borehole (depths 225.7–218.5 m), Leningrad region, Russia; Staraya Russa Formation, Redkino Group, Upper Vendian, Ediacaran (Kushim *et al.* 2016; Golubkova *et al.* 2018). (3) Kunevichi-4 borehole (depth 557–558 m), Leningrad region, Russia; Staraya Russa Formation, Redkino Group, Upper Vendian, Ediacaran (Jensen, 2003). (4) Kepina-775 borehole, Arkhangelsk region, Russia; Lyamtsa Formation, Valdai Group, Upper Vendian, Ediacaran (pers. obs.). (5) Onega Peninsula, Lyamtsa River, Arkhangelsk region, Russia; Lyamtsa and Verkhovka formations, Valdai Group, Upper Vendian, Ediacaran (pers. obs.). (6) Onega Peninsula, Solza River, Arkhangelsk region, Russia; Verkhovka Formation, Valdai Group, Upper Vendian, Ediacaran (pers. obs.). (7) Onega Peninsula, Syuzma River, Arkhangelsk region, Russia; Verkhovka Formation, Valdai Group, Upper Vendian, Ediacaran (pers. obs.). (8) South Urals, Tramshak River, Republic of Bashkortostan, Russia; Basa Formation, Asha Group, Upper Vendian, Ediacaran (pers. obs.). (9) Transndniester Podolia, Khmelnitskyi region, Ukraine; Mogilev Formation, Mogilev–Podolsky Group, Upper Vendian, Ediacaran (*sensu* Fedonkin, 1983).

https://doi.org/10.1017/S0016756822000437 Published online by Cambridge University Press

(10) South Urals, Inzer River, Republic of Bashkortostan, Russia; Basa Formation, Asha Group, Upper Vendian, Ediacaran (pers. obs.). (11) Dorogobuzh borehole (depths 881–873 m), Smolensk region, Russia; Nelidovo Formation, Redkino Group, Upper Vendian, Ediacaran (Gnilovskaya, 1985, 1990).

Material. 47 specimens.

Remarks. Orbisiana spumea is a new taxon represented by a foam-like aggregation of globular chambers, with a wide chronostratigraphic distribution within the East European Platform. It has previously been described under a variety of informal names, such as: 'assemblage of coprolites' (in Fedonkin, 1983, p. 161, pl. XXXIV, fig. 5), 'mass of coprolites' (in Chistyakov *et al.* 1984, p. 13, fig. 2m), 'assemblage of small globular coprolites' (in Fedonkin, 1985, p. 206, pl. XXII, fig. 3), 'accumulations of fine round coprolites' (in Fedonkin, 1990, p. 268, pl. 22, fig. 3), '*Neonereites*, strings of fecal pellets' (in Fedonkin *et al.* 2007, p. 208, fig. 402) and unnamed form (in Fedonkin *et al.* 2007, p. 210, fig. 405). All mentioned occurrences satisfy the specific diagnosis of *Orbisiana spumea* in terms of morphology.

Genus *Palaeopascichnus* Palij, 1976

1976 *Palaeopascichnus* Palij, p. 74.

1980 *Intrites* Fedonkin, p. 44.

1985 *Yelovichnus* Fedonkin, p. 207.

1989 *Catellichnus* Becker & Kishka, pp. 118–19.

2013 *Catellichnus* Becker, p. 62.

2013 *Iterichnus* Becker, pp. 60–1.

2013 *Palaeopascichnus* Becker, p. 71.

2013 *Pseudobergaueria* Becker. p. 74.

Type species. Palaeopascichnus delicatus Palij, 1976

Species composition. Palaeopascichnus delicatus, *P. linearis* and *P. gracilis*.

Original description. A system of trace fossils represented by densely spaced parallel fine grooves (in negative epirelief). The grooves are split to the edge, their terminations are obscure or blunt. The positive hyporelief is formed by narrow densely spaced parallel rolls (translated here, after the Russian diagnosis provided in Palij, 1976).

Revised diagnosis. Recumbent colonial agglutinated chambered organisms. Chambers are globular or elongated; they are organized in series that branch repeatedly. Width and/or length of chambers can be consistent with each specimen, but in most cases it is gradually increasing at various rates.

Remarks. Initially, V.M. Palij diagnosed genus *Palaeopascichnus* as ancient trace fossils (Palij, 1976). Over several decades, these forms were interpreted as traces of movement or accumulation of coprolites. The diagnosis of *Palaeopascichnus delicatus* was emended by Shen *et al.* (2007), who improperly applied the diagnosis of species *Palaeopascichnus delicatus* instead of that for the genus *Palaeopascichnus* (Palij, 1976); in addition, they referred to Palij *et al.* (1979), which was published later than the original work of Palij (1976). Shen *et al.* (2007) described the new species *Palaeopascichnus minimum* and *P. meniscatus*, which however differ significantly from classic palaeopascichnid fossils. These fossils, together with *Palaeopascichnus wangjiawanensis* Yin and *P. jiumenensis* Dong, bear a striking resemblance to representatives of the ichnogenus *Nenoxites* Fedonkin (Rogov *et al.* 2012, 2013*a*, *b*; Luo & Miao, 2020). It is suggested here that these ichnofossils be eliminated from the genus *Palaeopascichnus* and species composition be restricted to *Palaeopascichnus delicatus*, *P. gracilis* and *P. linearis*. Genera *Catellichnus*, *Intrites* and *Yelovichnus* were revised by Jensen *et al.* (2006) and reinterpreted as palaeopascichnid-like fossils, but without any systematic description. The same informal revision was performed by Kolesnikov *et al.* (2015) for the genera *Catellichnus*, *Iterichnus*, *Palaeopascichnus* and *Pseudobergaueria*, where such fossils were interpreted as agglutinated macroscopic organisms of unknown affinity but without any systematic palaeontology. It is worth noting a recently described 'modular fossil' *Curviacus ediacaranus* Shen, which is considered as a palaeopascichnid-like fossil (Shen *et al.* 2017), but in some degree it is similar to the ichnofossil *Nenoxites* (in thin-section it displays menisc-like texture), and the palaeopascichnid affinity of this problematic fossil is controversial (Kolesnikov *et al.* 2018*a*, *b*; Liu & Tindal, 2020; Peng *et al.* 2020; Wan *et al.* 2020). In particular, it has significantly wide and curved units and some of them have conical projections (Shen *et al.* 2017; Jensen *et al.* 2018). Thus, it is not considered by us to represent a palaeopascichnid organism.

Palaeopascichnus delicatus Palij (1976) (Figs 2a, c, 3a–e, h)

1976 *Palaeopascichnus delicatus* Palij, p. 192, pl. XXIV, fig. 2.

1985 *Palaeopascichnus delicatus* Fedonkin, p. 206, pl. XXII, fig. 1.

1990 *Palaeopascichnus delicatus* Fedonkin, p. 340, pl. 22, fig. 1.

1995 *Palaeohelminthoida* sp. Jenkins, p. 57, pl. 2., fig. i (*partim*).

2009 *Palaeopascichnus* Gehling & Droser, p. 204, fig. 7a, c.

2010 *Nereites irregularis* Becker, p. 28, pl. II, fig. 1.

2010 *Flexorhaphe crassa* Becker, p. 28, pl. II, fig. 2.

2010 'palaeopascichnids' Grazhdankin *et al.* p. 43, fig. 24d.

2013 *Diplichnites* Becker, p. 58, pl. I, fig. 11 (*partim*).

2013 *Helminthorhaphe miocenica* Becker, p. 58, pl. I, fig. 16 (*partim*).

2013 *Nereites irregularis* Becker, p. 72, pl. III, fig. 2 (*partim*).

2013 *Pseudobergaueria bashkirikus* Becker, p. 72, pl. III, fig. 10.

2013 *Steinfjordichnus brutoni* Becker, p. 72, pl. III, fig. 12.

2014 *Palaeopascichnus delicatus* Grazhdankin, p. 270, fig. 1-1.

2015 *Palaeopascichnus delicatus* Ivantsov *et al.* p. 135, pl. VI, fig. 7.

2015 'palaeopascichnids' Kolesnikov *et al.* p. 72, fig. 9G, H.

2018 *Palaeopascichnus delicatus* Jensen *et al.* p. 5, fig. 3A (*partim*).

2018 *Punctorhaphe parallela* Ivantsov *et al.* p. 184, pl. VIII, fig. 7.

2018 *Pseudobergaueria bashkirikus* Ivantsov *et al.* p. 187, pl. X, fig. 1.

2018 *Helminthorhaphe miocenica* Ivantsov *et al.* p. 187, pl. X, fig. 5.

2019 *Palaeopascichnus delicatus* Kolesnikov, p. 3, fig. 1A.

2021 *Palaeopascichnus delicatus* Desiatkin *et al.* p. 644, fig. 1d–f.

Holotype. Specimen No. 1907/7 (Fig. 3a) stored in the National Museum of Natural History (NMNH NASU), Kiev, Ukraine (Ivantsov *et al.* 2015, p. 135, pl. VI, fig. 7).

Type locality. Middle Dniester area, right bank of Dniester River, Molodovo village, Ediacaran Kanilovka Group, Komarovo Beds, Khmelnitsky region, Ukraine.

Original description. Negative epirelief represents the series of parallel, in most cases arcuate, small furrows that are closely abutted to each other, with corresponding low ridges in positive hyporelief. The surface shape of ridges is arcuate in cross-section, their endings are indistinct, gradually passing into rock surface or rounded. In some cases, transverse segmentation of ridges by constrictions is observed. The number of furrows in one series ranges from four to ten and more (translated here, after the Russian diagnosis provided in Palij, 1976).

Emended diagnosis. Test agglutinated, elongated, curved or rectilinear, branched occasionally, consisting of a single series of variously elongated ellipsoidal chambers. Width and/or length

https://doi.org/10.1017/S0016756822000437 Published online by Cambridge University Press

increases successively within each individual chamber. Chamber shape varies from smaller globular in the initial chamber and larger allantoid or extremely elongated crescent- and arc-like in the last one.

Occurrence. (1) Digermulen Peninsula, Finnmark, Norway; Manndraperelva Member of the Stahpogieddi Formation, Ediacaran (McIlroy & Brasier, 2016; Jensen *et al.* 2018). (2) Onega Peninsula and Winter Coast, White Sea area, Arkhangelsk region, Russia; Verkhovka and Lyamtsa formations, Valdai Group, Upper Vendian, Ediacaran (Fedonkin, 1985, 1990). (3) Sylvitsa River and Lake Shirokovskoye, Central Urals, Sverdlovsk and Perm regions, Russia; Siniy Kamen Member, Chernyi Kamen Formation, Perevalok Formation, Sylvitsa Group, Upper Vendian, Ediacaran (Grazhdankin *et al.* 2010; Desiatkin *et al.* 2021). (4) Flinders Ranges, East Kimberley, Australia; Wonoka Formation, Ediacaran (Gehling *et al.* 2000). (5) Malyi Ryauzyak River, South Urals, Republic of Bashkortostan, Russia; Basa Formation, Asha Group, Upper Vendian, Ediacaran (Becker, 2013; Kolesnikov *et al.* 2015). (6) Avalon Peninsula, Newfoundland, Canada; Fermeuse and Trepassey formations, Ediacaran (Hawco *et al.* 2019). (7) Tuchkino-1000 borehole, Arkhangelsk region, Russia; Lyamtsa Formation, Valdai Group, Upper Vendian, Ediacaran (pers. obs.). (8) Olenek Uplift, NE Siberia, Russia; Khatyspyt Formation, Khorbusuonka Group, Upper Vendian, Ediacaran (Nagovitsin *et al.* 2015; Kolesnikov *et al.* 2018*a*).

Material. 58 specimens.

Remarks. Palaeopascichnus delicatus Palij was described from the Ediacaran deposits in Podolia (Ukraine); however, similar objects had been discovered earlier in Australia, but without formal description (Glaessner, 1969). It also is on the list of ichnofossils from the Lublin region of Poland; however, displayed photographically it resembles a *Nenoxites*-like meniscate structure (Paczesna, 1986).

Palaeopascichnus gracilis comb. nov. (Fig. 3f–h)

1985 *Yelovichnus gracilis* Fedonkin, p. 207, pl. XXVII, fig. 2.

1990 *Yelovichnus gracilis* Fedonkin, p. 340, pl. 27, fig. 2.

2000 *Yelovichnus gracilis* Gehling *et al.* p. 445, pl. 1, fig. 1.

2013 *Punctorhaphe parallela* Becker, p. 72, pl. III, fig. 11 (*partim*).

2013 *Flexorhaphe crassa* Becker, p. 58, pl. I, fig. 14 (*partim*).

2018 '*Yelovichnus*-type forms' Jensen *et al.* p. 5, figs 3A, 4C (*partim*).

2018 *Flexorhaphe crassa* Ivantsov *et al.* p. 187, pl. X, fig. 2.

2019 *Yelovichnus gracilis* Kolesnikov, p. 3, fig. 1C (*partim*).

2021 *Yelovichnus gracilis* Desiatkin *et al.* p. 644, fig. 1g–i.

Holotype. Specimen No. 3993/1309 (Fig. 3f) stored in the Borissyak Palaeontological Institute of the Russian Academy of Sciences (PIN RAS) in Moscow, Russia (Fedonkin, 1985, p. 207, pl. XXVII, fig. 2).

Type locality. Near the mouth of Yelovyi Creek, Winter Coast of the White Sea, Arkhangelsk region, NW Russia.

Original description. Narrow trace (positive hyporelief) represented by wide curve-like meanders; each transversal track within the series has an irregular wave-like trajectory; nevertheless, due to the regular bearing of the transversal tracks within a feeding direction, there is no empty space between the tracks (translated here, after the Russian diagnosis provided in Fedonkin, 1985, p. 207).

Emended diagnosis. Test agglutinated, elongated, curved or rectilinear, branched occasionally, consisting of a single series of significantly elongated sausage-shaped chambers. Width and/or length are relatively consistent within each individual chamber, but occasionally they are gradually increasing or decreasing.

Occurrence. (1) Digermulen Peninsula, Finnmark, Norway; Indreelva Member of the Stahpogieddi Formation, Ediacaran (McIlroy & Brasier, 2016; Jensen *et al.* 2018). (2) Winter Coast, White Sea area, Arkhangelsk region, Russia; Verkhovka and Lyamtsa formations, Valdai Group, Upper Vendian, Ediacaran (Fedonkin, 1985, 1990). (3) Sylvitsa River and Shirokovskoye Lake, Central Urals, Sverdlovsk and Perm regions, Russia; Siniy Kamen Member, Chernyi Kamen Formation, Sylvitsa Group, Upper Vendian, Ediacaran (Grazhdankin *et al.* 2010; Desiatkin *et al.* 2021). (4) Flinders Ranges, East Kimberley, Australia; Wonoka Formation, Ediacaran (Gehling *et al.* 2000). (5) Malyi Ryauzyak River, South Urals, Republic of Bashkortostan, Russia; Basa Formation, Asha Group, Upper Vendian, Ediacaran (Becker, 2013; Kolesnikov, 2019). (6) Avalon Peninsula, Newfoundland, Canada; Trepassey and Fermeuse formations, St John's Group, Ediacaran (Hawco *et al.* 2019).

Material. 33 specimens.

Remarks. Yelovichnus gracilis was initially described as a meandering trace fossil; however, it displays a strong resemblance to the palaeopascichnid fossils (Jensen, 2003; Jensen *et al.* 2006; McIlroy & Brasier, 2016; Hawco *et al.* 2019). It was also suggested recently from the study of a new fossil material from the Digermulen Peninsula, Norway (Jensen *et al.* 2018). Thus we consider it as *Palaeopascichnus gracilis* comb. nov. It is interesting to note a superficial similarity to some representatives of *Yangtziramulus zhangi* from the lower Shibantan Member in the Yangtse Gorges area, China, (Xiao *et al.* 2020) with taxon *Palaeopascichnus gracilis*. However, Xiao *et al.* (2020) described several completely preserved specimens of *Yangtziramulus zhangi* which show branch- and tree-like structures instead of the typical chain-like chambered bodies in palaeopascichnid fossils.

Palaeopascichnus linearis Fedonkin, 1976 (text-pl., figs 2, 3)

For earlier synonymy see Kolesnikov *et al.* (2018*a*).

2017 *Palaeopascichnus* sp. Ivantsov, p. 145, fig. 2c.

2018 *Palaeopascichnus renarius* Ivantsov, p. 1338, pl. 1, figs 8–9.

2018 *Neonereites uniserialis* Ivantsov *et al.* p. 183, pl. VIII, fig. 7.

2018 *Palaeopascichnus delicatus* Ivantsov *et al.* p. 185, pl. IX, fig. 3.

2018 *Iterichnus ternarius* Ivantsov *et al.* p. 185, pl. IX, figs 2, 4.

2018 *Chondrites targionii* Ivantsov *et al.* p. 185, pl. IX, fig. 5.

2018 *Tuapseichnium radialis* Ivantsov *et al.* p. 185, pl. IX, fig. 6.

2018 *Neonereites renarius* Ivantsov *et al.* p. 187, pl. X, fig. 3.

2018 *Diplichnites* sp. Ivantsov *et al.* p. 187, pl. X, fig. 4.

2018 *Steinsfjordichnus turbidis* Ivantsov *et al.* p. 187, pl. X, fig. 6.

2018 *Steinsfjordichnus brutoni* Ivantsov *et al.* p. 187, pl. X, fig. 7.

2018 *Helminthorhaphe miocenica* Ivantsov *et al.* p. 187, pl. X, fig. 6.

2018 *Palaeopascichnus delicatus* Jensen *et al.* p. 5, fig. 3B, C, D.

2018 *Palaeopascichnus delicatus* Jensen *et al.* p. 5, fig. 4A, B.

2018 *Palaeopascichnus linearis* Kolesnikov *et al.* pp. 26–33, figs 2A–C, 3A, D, 4A, 5A–B, 9A–E, 10A, 11A.

2019 *Palaeopascichnus* Hawco *et al.* pp. 4–5, figs 4A–C, 5A–D.

2019 *Palaeopascichnus linearis* Kolesnikov, p. 3, fig. 1B.

2019 *Palaeopascichnus linearis* Kolesnikov, p. 3, fig. 1C (*partim*).

2021 *Palaeopascichnus linearis* Desiatkin *et al.* p. 644, fig. 1j–l.

Holotype. Specimen No. GIN 4310/8-5 stored in the Borissyak Palaeontological Institute of the Russian Academy of Sciences in Moscow (PIN RAS), Russia (Fedonkin, 1976, text-figs 2, 3).

Type locality. Approximately 5.7 km upstream of the mouth of Syuzma River, Onega Peninsula, SE White Sea area, *c.* 80 km west of Arkhangelsk, NW Russia.

https://doi.org/10.1017/S0016756822000437 Published online by Cambridge University Press

Diagnosis. Test agglutinated, elongated, curved or rectilinear, occasionally branching, consists of a single series of globular or ellipsoidal chambers 1–15 mm in width. The series occasionally diverge dichotomously. Chambers are relatively consistent in size within a series or gradually increase in width before diverging, but the length-to-width ratio of the chambers is relatively constant along the series. The wall thickness does not exceed 1 mm. Number of chambers in a series ranges between 3–5 and several dozens. The diagnosis is taken from Kolesnikov *et al.* (2018*a*).

Occurrence. (1) Xiuning and Yixian counties, Anhui Province, South China; Member 2 of the Lantian Formation, Ediacaran (Yuan *et al.* 2011; Wan *et al.* 2014). (2) Tuchkino-1000 borehole, Arkhangelsk region, Russia; Lyamtsa Formation, Valdai Group, Upper Vendian, Ediacaran (Golubkova *et al.* 2018). (3) Ferryland, Avalon Peninsula, Newfoundland, Canada; Trepassey and Fermeuse formations, St John's Group, Ediacaran (Hawco *et al.* 2019). (4) Olenek Uplift, NE Siberia, Russia; Khatyspyt Formation, Khorbusuonka Group, Upper Vendian, Ediacaran (Nagovitsin *et al.* 2015; Kolesnikov *et al.* 2018*a*). (5) SE White Sea area, Arkhangelsk region, Russia; Lyamtsa, Verkhovka, Zimnie Gory and Erga formations, Valdai Group, Upper Vendian, Ediacaran (Fedonkin, 1976, 1985; Fedonkin *et al.* 2007; Kolesnikov *et al.* 2018*a*). (6) Digermulen Peninsula, Finnmark, Norway; Manndraperelva Member, Stahpogieddi Formation, Ediacaran (McIlroy & Brasier, 2016; Jensen *et al.* 2018). (7) Sylvitsa River and Shirokovskoye Lake, Central Urals, Sverdlovsk and Perm regions, Russia; Perevalok and Chernyi Kamen formations, Sylvitsa Group, Upper Vendian, Ediacaran (Grazhdankin *et al.* 2010; Desiatkin *et al.* 2021). (8) Transdniester Podolia, SW Ukraine; Mohyliv and Studenitsa formations, Mohyliv–Podilskyi Group, Upper Vendian, Ediacaran (Fedonkin, 1985, 1990). (9) South Wales, United Kingdom; Coomb Volcanic Formation, Ediacaran (Cope, 1982). (10) Yudoma River, Uchur-Maya Basin, border between Khabarovsk region and Republic of Sakha (Yakutia), Russia; Ust-Yudoma Formation, Upper Vendian, Ediacaran (Ivantsov, 2017). (11) Flinders Ranges, South Australia; Ediacara Member, Rawnsley Quartzite, Pound Subgroup and Wonoka Formation, Ediacaran (Haines, 2000; Gehling & Droser, 2009). (12) Burin Peninsula, Newfoundland, Canada; Chapel Island Formation, St John's Group, Ediacaran (Narbonne *et al.* 1987). (13) South Urals, Republic of Bashkortostan and Chelyabinsk region, Russia; Basa and Zigan formations, Asha Group, Upper Vendian, Ediacaran (Becker, 2010, 2013; Kolesnikov *et al.* 2015, 2018*a*; Kolesnikov, 2019). (14) Tethys Himalaya, India; Debsakhat Member, Kuzum La Formation, Ediacaran (Parcha & Pandey, 2011).

Material. 943 specimens.

Remarks. The interpretation and research history of *Palaeopascichnus linearis* was discussed in detail in Kolesnikov *et al.* (2018*a*). The report *Palaeopascichnus linearis* from India of Ediacaran age is unclear because it is accompanied by a number of Cambrian trace fossils (Parcha & Pandey, 2011). The other possibility is that the incompletely preserved specimen is not *Palaeopascichnus linearis*. Also, there is one specimen of *Palaeopascichnus* from India only.

5. Discussion

That palaeopascichnid fossils are in need of a revision has long been thought (Jensen, 2003; Seilacher *et al.* 2003; Antcliffe *et al.* 2011; Grazhdankin, 2014; Jensen *et al.* 2018; Kolesnikov *et al.* 2018*a*, *b*; Hawco *et al.* 2019; Kolesnikov, 2019), but the global abundance and complicated interpretations have made it difficult to differentiate species. In the present study we have integrated morphometric data, stratigraphic distribution and depositional settings of more than 1200 specimens of Palaeopascichnida worldwide. On the one hand, the PCA test of chamber shape within *Palaeopascichnus* displays a wide variability (Fig. 6) and also supports the idea of separation of measured specimens into three clusters. On the other hand, it contradicts the developing rules proposed by Antcliffe *et al.* (2011), who reported that chamber width was always greater than length. We interpret the three statistically supported clusters as different morphotypes, representing separate species in the genus: *Palaeopascichnus gracilis*, *P. delicatus and P. linearis*. All of them demonstrate a marked difference in palaeoenvironmental optimum and tolerance range in the sedimentary environments (Fig. 7). *P. delicatus* and *P. gracilis* show almost the same environmental optimum in transitional shallow water and marine facies, although the former has a wider tolerance range limited by continental (tidal flat) and carbonate (shallow open marine) facies. It is also worthy of note that these species are not as abundant as the taxon *P. linearis*, the environmental optimum of which is shifted to relatively deeper depositional settings. We do not know yet if this pattern is real, or if it can be explained by selective sampling of fossil material, taphonomic window effect or absence of additional data. However, if these organisms had an agglutinated skeleton and the widest palaeogeographical distribution among the Ediacaran macroscopic biota (Seilacher *et al.* 2003; Antcliffe *et al.* 2011; Grazhdankin, 2014; Kolesnikov *et al.* 2018*a*, *b*; Hawco *et al.* 2019), the first results of study of palaeoenvironmental distribution are to some extent reliable.

The recent discoveries of agglutinated skeleton in *Palaeopascichnus* and *Orbisiana* also place emphasis on this group of extinct organisms in terms of biostratigraphic significance for the Ediacaran and terminal Ediacaran–Cambrian sequences (Kolesnikov, 2019). An example of the potential use of palaeopascichnids in stratigraphical and geological correlation is found in the proposal of Grazhdankin & Maslov (2015) for the 'Vendian Series' as a candidate upper series of the Ediacaran System. Grazhdankin & Maslov (2015) suggested that the 'Vendian Series' can be subdivided into Laplandian, Redkinian, Belomorian and Kotlinian stages which are typified by regional stratigraphic units of the Vendian sedimentary sequences of the East European Platform. *Palaeopascichnus linearis* is probably the only species meeting the criterion of a 'Vendian Series' index-taxon whose stratigraphic range spans almost the entire series (Fig. 1). The oldest representatives of this species are found in Member 2 of the Lantian Formation in South China (Yuan *et al.* 2011), the minimum age of which constrained to 602 ± 7 Ma (Yang *et al.* 2022), and the youngest taxa occur in the uppermost part of the Ediacaran Zigan Formation in the South Urals, Russia (Kolesnikov, 2019; Kolesnikov & Bobkov, 2019), which also correlates to a similar level of the Cambrian Global Boundary Stratotype Section and Point (GSSP) in Newfoundland (Narbonne *et al.* 1987; Kolesnikov *et al.* 2015). The species *P. delicatus* and *P. gracilis* demonstrate a narrower stratigraphic range (Fig. 1), and they distributed mainly in 'Belomorian' and 'Kotlinian' stages (Grazhdankin, 2014; Kolesnikov, 2019; Desiatkin *et al.* 2021).

Orbisiana is known from the East European Platform only, and the three species demonstrate similar palaeoenvironmental optimum and tolerance range in sedimentary environments (Fig. 7). The oldest representatives of *Orbisiana simplex* and *Orbisiana*

https://doi.org/10.1017/S0016756822000437 Published online by Cambridge University Press

spumea are found in the lower parts of the Staraya Russa and Gavrilov Yam formations of the Redkino Group of the Ladoga and Moscow basins respectively (Golubkova *et al.* 2018; Kolesnikov *et al.* 2018*b*; Kolesnikov, 2019), which are attributed to the Redkinian regional stage of the Upper Vendian of the East European Platform (Grazhdankin & Maslov, 2015). The youngest specimens occur in the uppermost part of the Asha Group of the South Urals together with trace fossils of the ichnogenus *Didymaulichnus*, suggesting a correlation with Ediacaran–Cambrian boundary strata (Kolesnikov *et al.* 2015; Kolesnikov & Bobkov, 2019) and Kotlinian regional stage (Fig. 1). *Orbisiana intorta* is described from the Verkhovka Formation of the Valdai Group of the White Sea area (Onega Peninsula). At the present time this species is known from one fossil locality only, belonging to the Belomorian regional stage of the East European Platform. *Orbisiana* shows a relatively narrow bioprovinciality in the Ediacaran: a total of 187 specimens of *Orbisiana* are distributed within the East European Platform and most of them were found in boreholes. Taking into account that a borehole is a tiny spot in the huge platform, this suggests that *Orbisiana* occurred in high density in these shales. The stratigraphic potential of *Orbisiana* species is unclear, and at present it may be a working option for regional stratigraphic correlation of the Neoproterozoic within the East European Platform only.

Future research is obviously required to define and model the phylogenetic relationships between Ediacaran problematic modular and chain-like macrofossils: for example, comparison of the taxa *Palaeopascichnus* and *Orbisiana* to *Funisia dorothea* (Droser & Gehling, 2008) and *Harlaniella podolica* (Jensen, 2003), which consist of somewhat similar modules that might be series of chambers, and are found in association with Palaeopascichnida in Ediacaran sedimentary sequences. Also, particular attention should be given to the other problematic Ediacaran fossils: *Shaanxilithes ningqiangensis* from the Schwarzrand subgroup of Namibia (MacDonald *et al.* 2014; Darroch *et al.* 2016, 2021), consisting of a single, occasionally diverged and net-like series of modules, and '*Palaeopascichnus*' from the Itajaí Basin of Brazil (Becker-Kerber *et al.* 2020), which are both morphologically similar to *Harlaniella podolica* from Podolia, Ukraine.

6. Conclusions

Step by step the systematic classification of the Ediacaran biota is becoming clearer. The group Palaeopascichnida has been problematic for many years. An integrated morphological, statistical and palaeoecological approach provides a clear discrimination into species within the group: *Orbisiana intorta*, *O. simplex*, *O. spumea*, *Palaeopascichnus delicatus*, *P. gracilis* and *P. linearis*. They are some of the most abundant macroscopic Ediacaran skeletal fossils, and perhaps the only Ediacaran group of fossils that is potentially useful in the geological correlation and stratigraphic subdivision of the Ediacaran System. The new insights into the palaeoenvironmental distribution and taxonomy of *Palaeopascichnus* and *Orbisiana* provided herein are central to the identification of possible homologies between these genera, and should provide a robust framework for future classification of other Ediacaran chambered organisms and reconstruction of their phylogenies.

Supplementary material. To view supplementary material for this article, please visit https://doi.org/10.1017/S0016756822000437

Acknowledgements. The core of the study was funded by the Russian Science Foundation (grant No. 21-77-10106). Large image processing and interpretation of photographs of the palaeopascichnids was supported by the Ministry of Education and Science of Russia (megagrant No. 075-15-2019-1883). The study was carried out on the state assignment of the Geological Institute RAS. Dima Grazhdankin (Novosibirsk), Elena Golubkova (St Petersburg) and Alex Liu (Cambridge, UK) generously shared their knowledge and photographs of palaeopascichnids from the East European Platform and Australia. We thank our two reviewers, Andrey Zhuravlev and Charlotte Kenchington, whose comments and remarks greatly improved the paper. We also thank Sören Jensen for his helpful comments and suggestions on the earlier and final drafts of this paper.

Conflict of interest. The authors declare that there is no conflict of interest.

References

Alve E and Goldstein ST (2010) Dispersal, survival and delayed growth of benthic foraminiferal propagules. *Journal of Sea Research* **63**, 36–51.

Antcliffe JB, Gooday AJ and Brasier MD (2011) Testing the protozoan hypothesis for Ediacaran fossils: a developmental analysis of *Palaeopascichnus*. *Palaeontology* **54**, 1157–75.

Becker YuR (2010) Geologitcheskii potentsial drevnikh ikhnofossilii v stratotipe pozdnego dokembriya Yuzhnogo Urala. *Regionalnaya Geologiya i Metallogeniya* **43**, 18–35 (in Russian).

Becker YuR (2013) Ichnofossils – a new paleontological object in the late Precambrian stratotype of the Urals. *Litosfera* **1**, 52–80.

Becker YuR and Kishka NV (1989) Discovery of the Ediacaran biota in the South Urals. In *Theoretical and Applied Aspects of Modern Paleontology* (eds TN Bogdanova & LI Khozatsky), pp. 109–20. Proceedings of the XXXIII Session of the All-Union Paleontological Society. Leningrad: Nauka.

Becker-Kerber B, Paim PSG, Junior FC, Girelli TJ, Zucatti da Rosa AL, El Albani A, Oses GL, Prado GMEM, Figueiredo M, Simoes LSA and Pacheco MLAF (2020) The oldest record of Ediacaran macrofossils in Gondwana (~563 Ma, Itajaí Basin, Brazil). *Gondwana Research* **84**, 211–28.

Bobkov NI, Kolesnikov AV, Maslov AV and Grazhdankin DV (2019) The occurrence of *Dickinsonia* in non-marine facies. *Estudios Geologicos* **75**, e096.

Chistyakov BG, Kalmykova NA, Nesov LA and Suslov GA (1984) O nalitchii vendskikh otlozhenii v srednem tetchenii r. Onegi i vozmozhnom suschestvovanii obolotchnikov (Tinicata: Chordata) v dokembrii. *Vestnik Leningradskogo Universiteta, Seriya Geologicheskaya* **6**, 11–19 (in Russian).

Cope JCW (1982) Precambrian fossils of the Carmarthen area, Dyfed. *Nature in Wales* n.s. **1**, 11–6.

Darroch SAF, Boag TH, Racicot RA, Tweedt S, Mason SJ, Erwin DH and Laflamme M (2016) A mixed Ediacaran–Metazoan assemblage from the Zaris Sub-basin, Namibia. *Palaeogeography, Palaeoclimatology, Palaeoecology* **459**, 198–208.

Darroch SAF, Cribb AT, Buatois LA, Germs GJB, Kenchington CG, Smith EF, Mocke H, O'Neil GR, Schiffbauer JD, Maloney KM, Racicot RA, Turk KA, Gibson BM, Almond J, Koester B, Boag TH, Tweedt SM and Laflamme M (2021) The trace fossil record of the Nama Group, Namibia: exploring the terminal Ediacaran roots of the Cambrian explosion. *Earth-Science Reviews* **212**, 103435.

Desiatkin VD, Kolesnikov AV, Rimsky AA, Sysoeva AO, Terekhova VA, Kuzntestov NB, Shazillo AV, Latysheva IV, Romanyuk TV and Fedonkin MA Palaeopascichnids from the Upper Vendian Chernyi Kamen Formation of the Middle Urals (Perm Region). *Doklady Earth Sciences* **499**, 643–7.

Dillon WR and Goldstein M (1984) *Multivariate Analysis: Methods and Applications*. Chichester: Wiley, 608 pp.

Droser ML and Gehling JG (2008) Synchronous aggregate growth in an abundant new ediacaran tubular organism. *Science* **319**, 1660–62.

Fedonkin MA (1976) Sledy mnogokletotchnykh iz valdaiskoi serii. *Izvestiya Akademii Nauk SSSR, Seriya Geologicheskaya* **4**, 129–32 (in Russian).

Fedonkin MA (1980) Iskopaemye sledy dokembriiskikh Metazoa. *Izvestiya Akademii Nauk SSSR, Seriya Geologicheskaya* **1**, 39–46 (in Russian).

Fedonkin MA (1981) White Sea biota of Vendian: Precambrian non-skeletal fauna in the Russian Platform North. In Transactions of the Geological Institute, vol. 342 (ed BM Keller), pp. 1–100, Moscow: Nauka.

Fedonkin MA, Gehling JG, Grey K, Narbonne GM and Vickers-Rich P (2007) *The Rise of Animals: Evolution and Diversification of the Kingdom Animalia*. Baltimore: Johns Hopkins University Press, 326 pp.

Fedonkin MA (1985) Palaeoichnology of Vendian Metazoa. In *The Vendian System: Substantiation from the Perspective of Historical Geology and Palaeontology* (eds BS Sokolov & AB Iwanowski), pp. 112–7. Moscow: Nauka.

Fedonkin MA (1990) Palaeoichnology of Vendian Metazoa. In *The Vendian System, vol. 1, Paleontology* (eds BS Sokolov and AB Iwanowski), pp. 132–7. Berlin and Heidelberg: Springer-Verlag.

Fedonkin MA (1983) Non-skeletal fauna of Podolia, Dniester Valley. In *The Vendian of Ukraine* (eds VA Velikanov, EA Aseeva & MA Fedonkin), pp. 128–39. Kiev: Naukova Dumka.

Gehling JG and Droser ML (2009) Textured organic surfaces associated with the Ediacara biota in South Australia. *Earth-Science Reviews* **96**, 196–206.

Gehling JG, Droser ML, Jensen S and Runnegar BN (2005) Ediacara organisms: relating form to function. In *Evolving Form and Function: Fossils and Development* (ed. DEG Briggs), pp. 43–6. Proceedings of a symposium honouring Adolph Seilacher for his contributions to palaeontology in celebration of his 80th birthday. New Haven: Peabody Museum of Natural History, Yale University.

Gehling JG, Narbonne GM and Anderson MM (2000) The first named Ediacaran body fossil, *Aspidella terranovica*. *Palaeontology* **43**, 427–546.

Glaessner M (1969) Trace fossils from the Precambrian and basal Cambrian. *Lethaia* **2**, 369–93.

Gnilovskaya MB (1985) Vendotaenids – Vendian Metaphyta. In *The Vendian System: Substantiation from the Perspective of Historical Geology and Palaeontology* (eds BS Sokolov & AB Iwanowski), pp. 117–25. Moscow: Nauka.

Gnilovskaya MB (1990) Vendotaenids – Vendian Metaphyta. In *The Vendian System, Vol. 1, Paleontology* (eds BS Sokolov and AB Iwanowski), pp. 138–48. Berlin and Heidelberg: Springer-Verlag.

Golubkova EYu, Kushim EA, Kuznetsov AB, Yanovskii AS, Maslov AV, Shvedov SD and Plotkina YuV (2018) Redkinian biota of macroscopic fossils from the Northwestern East European Platform (South Ladoga region). *Doklady Earth Sciences* **479**, 300–4.

Grazhdankin D (2014) Patterns of evolution of the Ediacaran soft-bodied biota. *Journal of Paleontology* **88**, 269–83.

Grazhdankin DV, Balthasar U, Nagovitsin KE and Kochnev BB (2008) Carbonate- hosted Avalon-type fossils in Arctic Siberia. *Geology* **36**, 803–6.

Grazhdankin DV and Maslov AV (2015) The room for the Vendian in the International Chronostratigraphic Chart. *Russian Geology and Geophysics* **56**, 549–59.

Grazhdankin DV, Maslov AV, Krupenin MT and Ronkin YuL (2010) *Depositional Systems of the Sylvitsa Group (Upper Vendian of the Central Urals)*. Ekaterinburg: UrO RAN, 280 pp.

Guisan A, Edwards TC and Hastie JT (2002) Generalized linear and generalized additive models in studies of species distributions: setting the scene. *Ecological Modelling* **157**, 89–100.

Haines PW (2000) Problematic fossils in the late Neoproterozoic Wonoka Formation, South Australia. *Precambrian Research* **100**, 97–108.

Hastie TJ and Tibshirani RJ (1986) Generalized additive models. *Statistical Science* **1**, 297–318.

Hawco JB, Kenchington CG and McIlroy D (2019) A quantitative and statistical discrimination of morphotaxa within the Ediacaran genus *Palaeopascichnus*. *Papers in Palaeontology* 7, 657–73. doi: 10.1002/spp2.1290.

Högström AES, Jensen S, Palacios T and Ebbestad JOR (2013) New information on the Ediacaran-Cambrian transition in the Vesteranda Group, Finnmark, northern Norway, from trace fossils and organic-walled microfossils. *Norwegian Journal of Geology* **93**, 95–106.

Ivantsov AYu (2017) Finds of Ediacaran-type fossils in Vendian deposits of the Yudoma Group, eastern Siberia. *Doklady Earth Sciences* **472**, 143–6.

Ivantsov AYu (2018) Vendian macrofossils of the Yudoma Group, southeast of the Siberian Platform. *Paleontological Journal* **52**, 1335–46.

Ivantsov AYu, Gritsenko VP, Paliy VM, Velikanov VA, Konstantinenko LI, Menasova ASh, Fedonkin MA, Zakrevskaya MA and Serezhnikova EA (2015) *Upper Vendian Macrofossils of Eastern Europe. Middle Dniester Area and Volhynia*. Moscow: PIN RAS, 144 pp.

Ivantsov AYu, Razumovskiy AA and Zakrevskaya MA (2018) *Upper Vendian Macrofossils of Eastern Europe. Middle and Southern Urals*. Moscow: PIN RAS, 190 pp.

Jenkins RJF (1995) The problems and potential of using animal fossils and trace fossils in terminal Proterozoic biostratigraphy. *Precambrian Research* **73**, 51–69.

Jensen S (2003) The Proterozoic and earliest Cambrian trace fossil record: patterns, problems and perspectives. *Integrative & Comparative Biology* **43**, 219–28.

Jensen S, Droser ML and Gehling JG (2006) A critical look at the Ediacaran trace fossil record. In *Neoproterozoic Geobiology and Paleobiology* (eds S Xiao and AJ Kaufman), pp. 115–57., Dordrecht: Springer.

Jensen S, Högström AES, Høyberget M, Meinhold G, McIlroy D, Ebbestad JOR, Taylor WL, Agic H and Palacios T (2018) New occurrences of *Palaeopascichnus* from the Stáhpogieddi Formation, Arctic Norway, and their bearing on the age of the Varanger Ice Age. *Canadian Journal of Earth Sciences* **55**, 1–10.

Kolesnikov AV (2019) Stratigraphic correlation potential of the Ediacaran palaeopascichnids. *Estudios Geologicos* **75**, e102.

Kolesnikov AV and Bobkov NI (2019) Revisiting the age of the Asha Group in the South Urals. *Estudios Geologicos* **75**, e103.

Kolesnikov AV, Liu AG, Danelian T and Grazhdankin DV (2018b) A reassessment of the problematic Ediacaran genus *Orbisiana* Sokolov 1976. *Precambrian Research* **316**, 197–205.

Kolesnikov AV, Marusin VV, Nagovitsin KE, Maslov AV and Grazhdankin DV (2015) Ediacaran biota in the aftermath of the Kotlinian Crisis: Asha Group of the South Urals. *Precambrian Research* **263**, 59–78.

Kolesnikov AV, Rogov VI, Bykova NV, Danelian T, Clausen S, Maslov AV and Grazhdankin DV (2018a) The oldest skeletal macroscopic organism *Palaeopascichnus linearis*. *Precambrian Research* **316**, 24–37.

Kushim EA, Golubkova EYu and Plotkina YuV (2016) Biostratigrafitcheskoe rastchlenenie vend-kembriiskikh otlozhenii Yuzhnogo Priladozhiya. *Vestnik Voronezhskogo Gosudarstvennogo Universiteta. Seriya: Geologiya* **4**, 18–22 (in Russian).

Liu AG and McIlroy D (2015) Horizontal surface traces from the Fermeuse Formation, Ferryland (Newfoundland, Canada), and their place within the late Ediacaran ichnological revolution. In *Ichnology: Publications Arising from ICHNIA III* (ed D McIlroy), pp. 141–56. St John's: Geological Association of Canada, Miscellaneous Publications, 9.

Liu AG and Tindal BH (2020) Ediacaran macrofossils prior to the ~580 Ma Gaskiers glaciation in Newfoundland, Canada. *Lethaia* **54**, 260–70.

Luo C and Miao L (2020) A Harodiskia-Nenoxites-dominated fossil assemblage from the Ediacaran-Cambrian transition (Liuchapo Formation, Hunan Province): its paleontological implications and stratigraphic potential. *Palaeogeography, Palaeoeclimatology, Palaeoecology* **545**, 109635.

MacDonald FA, Pruss SB and Strauss JV (2014) Trace fossils with Spreiten from the Late Ediacaran Nama Group, Namibia: complex feeding patterns five million years before the Precambrian-Cambrian boundary. *Journal of Paleontology* **88**, 299–308.

Martyshin A (2012) Ediacaran fauna from the Yampil Sandstones of the Vendian of Podolia. *Geolog Ukrainy* **4**, 97–104.

Mastitsky SE and Shitikov VK (2015) *Statistical Analysis and Data Visualisation using R*. Moscow: DMK Press, 496 pp.

McIlroy D and Brasier MD (2016) Ichnological evidence for the Cambrian explosion in the Ediacaran to Cambrian succession of Tanafjord, Finnmark, northern Norway. In *Earth System Evolution and Early Life: A Celebration of the Work of Martin Brasier* (eds AT Brasier, D McIlroy & N McLoughlin). Geological Society of London, Special Publication no. 448.

Mitchell EG, Bobkov NI, Bykova NV, Dhungana A, Kolesnikov AV, Hogarth IRP, Liu AG, Mustill TMR, Sozonov N, Rogov VI, Xiao S and Grazhdankin DV (2020) The influence of environmental setting on the community ecology of Ediacaran organisms. *Interface Focus* **10**, 20190109.

Murase H, Nagashima H, Yonezaki S, Matsukura R and Kitakado T (2009) Application of a generalized additive model (GAM) to reveal relationships

between environmental factors and distributions of pelagic fish and krill: a case study in Sendai Bay, Japan ICES. *African Journal of Marine Sciences* **66**, 1417–24.

Nagovitsin KE, Rogov VI, Marusin VV, Karlova GA, Kolesnikov AV, Bykova NV and Grazhdankin DV (2015) Revised Neoproterozoic and Terreneuvian stratigraphy of the Lena-Anabar Basin and north-western slope of the Olenek Uplift, Siberian Platform. *Precambrian Research* **270**, 226–45.

Narbonne GM, Myrow PM, Landing E and Anderson MM (1987) A candidate stratotype for the Precambrian-Cambrian boundary, Fortune Head, Burin Peninsula, south-eastern Newfoundland. *Canadian Journal of Earth Sciences* **24**, 1277–93.

Oksaken J, Blanchet GF, Friendly M, Kindt R, Legendre P, McGlinn D, Minchin PR, O'Hara RB, Simpson GL, Solymons P, Stevens MHH, Szoecs E and Wagner H (2020) *Vegan: Community Ecology Package. Version 2.5-7*. https://cran.r-project.org/web/packages/vegan/index.html.

Paczesna J (1986) Upper Vendian and Lower Cambrian ichnocoenoses of Lublin Region. *Biuletyn Instytutu Geologicznego* **355**, 31–47 (in Russian).

Palij VM (1976) Remains of soft-bodied animals and trace fossils from the Upper Precambrian and Lower Cambrian of Podolia. In *Palaeontology and Stratigraphy of Upper Precambrian and Lower Cambrian of Southwestern East European Platform* (eds BM Keller & AYu Rozanov), pp. 63–76. Kiev: Naukova Dumka.

Palij VM, Posti E and Fedonkin MA (1979) Soft-bodied Metazoa and animal trace fossils in the Vendian and early Cambrian. In Upper Precambrian and Cambrian Palaeontology of the East European Platform (eds BM Keller & AYu Rozanov), pp. 49–82. Moscow: Nauka (in Russian; English translation edited by. A Urbanek and AYu Rozanov, published in 1983 by Publishing House Wydawnictwa Geologiczne, Warsaw).

Parcha SK and Pandey S (2011) Ichnofossils and their significance in the Cambrian succession of the Parahio Valley in the Spiti Basin, Tethys Himalaya, India. *Journal of Asian Earth Sciences* **42**, 1097–116.

Peng Y, Dong L, Ma H, Wang R, Lang X, Peng Y, Qin S, Liu W and Shen B (2020) Surface ocean nitrate-limitation in the aftermath of Marinoan snowball Earth: evidence from the Ediacaran Doushantuo Formation in the western margin of the Yangtze Block, South China. *Precambrian Research* **347**, 105846.

Rogov V, Marusin V, Bykova N, Goy Y, Nagovitsin K, Kochnev B, Karlova G and Grazhdankin D (2012) The oldest evidence of bioturbation on Earth. *Geology* **40**, 395–8.

Rogov V, Marusin V, Bykova N, Goy Y, Nagovitsin K, Kochnev B, Karlova G and Grazhdankin D (2013a) The oldest evidence of bioturbation on Earth: REPLY. *Geology* **41**, e290.

Rogov V, Marusin V, Bykova N, Goy Y, Nagovitsin K, Kochnev B, Karlova G and Grazhdankin D (2013b) The oldest evidence of bioturbation on Earth: REPLY. *Geology* **41**, e300.

Runnegar B (1995) Vendobionta or Metazoa? Developments in understanding the Ediacara "fauna". *Neues Jahrbuch für Geologie und Paläontologie Abhandlungen* **195**, 303–18.

Seilacher A, Buatois L and Mangano MG (2005) Trace fossils in the Ediacaran-Cambrian transition: behavioral diversification, ecological turnover and environmental shift. *Palaeogeography, Palaeoclimatology, Palaeoecology* **227**, 323–56.

Seilacher A, Grazhdankin D and Legouta A (2003) Ediacaran biota: the dawn of animal life on the shadow of giant protists. *Paleontological Research* **7**, 43–54.

Seilacher A and Mrinjek E (2011) Benkovac Stone (Eocene, Croatia): a deep-sea Plattenkalk? *Swiss Journal of Geosciences* **104** (Supplement 1), 159–66.

Shen B, Xiao S, Dong L, Zhou C and Liu J (2007) Problematic macrofossils from Ediacaran successions in the North China and Chaidam Blocks: implications for their evolutionary roots and biostratigraphic significance. *Journal of Paleontology* **81** (6), 1396–1411.

Shen B, Xiao S, Zhou C, Dong L, Chang J and Chen Z (2017) A new modular palaeopascichnid fossil *Curviacus ediacaranus*: new genus and species from the Ediacaran Dengying Formation in the Yangtze Gorges area of South China. *Geological Magazine* **154**, 1257–68.

Sokolov BS (1976) Organic world of the Earth on its way to Phanerozoic differentiation. In *The 250th Anniversary of the Academy of Sciences of the USSR. Documents and Records of the Celebrations* (ed BS Sokolov), pp. 423–44. Moscow: Nauka.

Sozonov NG, Bobkov NI, Mitchell EG, Kolesnikov AV and Grazhdankin DV (2019) The ecology of *Dickinsonia* on tidal flats. *Estudios Geologicos* **75**, e116.

Waggoner B (2003) The Ediacaran biotas in space and time. *Integrative & Comparative Biology* **43**, 104–13.

Wan B, Chen Z, Yuan X, Pang K, Tang Q, Guan C, Wang X, Pandey SK, Droser ML and Xiao S (2020) A tale of three taphonomic modes: the Ediacaran fossil *Flabellophyton* preserved in limestone, black shale, and sandstone. *Gondwana Research* **84**, 296–314.

Wan B, Xiao S, Yuan X, Chen Z, Pang K and Tang Q (2014) Orbisiana linearis from the early Ediacaran Lantian Formation of South China and its taphonomic and ecological implications. *Precambrian Research* **255**, 266–75.

Wood SN (2006) *Generalized Additive Models: An Introduction with R*.Boca Raton: Chapman & Hall/CRC, 410 pp.

Xiao S, Chen Z, Pang K, Zhou C and Yuan X (2020) The Shibantan Lagerstätte: insights into Proterozoic-Phanerozoic transition. *Journal of the Geological Society* **178**, 1–12.

Yang C, Li Y, Selby D, Wan B, Guan C, Zhou C and Li XH (2022) Implications for Ediacaran biological evolution from the ca. 602 Ma Lantian biota in China. *Geology* **50**, 562–6.

Yuan X, Chen Z, Xiao S, Zhou C and Hua H (2011) An early Ediacaran assemblage of macroscopic and morphologically differentiated eukaryotes. *Nature* **470**, 390–3.

Zhuravlev AYu and Riding R (2000) *The Ecology of the Cambrian Radiation*. New York: Columbia University Press, 536 pp.

Zhuravlev AYu and Wood RA (2008) Eve of biomineralization: controls on skeletal mineralogy. Geology 36, 923–6.

https://doi.org/10.1017/S0016756822000437 Published online by Cambridge University Press